# NRC Publications Archive
# Archives des publications du CNRC

**Investigation of thermal performance of reflective insulations for different applications**
Saber, H. H.

National Research Council Canada    Conseil national de recherches Canada

Canada

# Investigation of thermal performance of reflective insulations for different applications

Saber, H.H.

National Research Council Canada

Conseil national de recherches Canada

Canada

# Investigation of Thermal Performance of Reflective Insulations for Different Applications

# Hamed H. Saber[*]

Institute for Research in Construction, National Research Council Canada

Bldg. M-24, 1200 Montreal Road, Ottawa, Ontario, Canada K1A 0R6

http://irc.nrc-cnrc.gc.ca/irccontents.html

## Abstract

Reflective insulations are being used in home attics, flat roofs, sloped roofs and wall systems of building envelopes. The present model, hygIRC-C, was used to investigate the contribution of the reflective insulations to the thermal resistance of specimens. The predictions of the present model were compared with test data of different sample stacks with different types of reflective insulations. In a previous study, the present model was benchmarked using test data obtained from a Guarded Hot Box (GHB) in accordance with the ASTM C-1363 test method. In this study, the test data was obtained from a different test method based on the heat flow meter in accordance of ASTM C-518 in the case of horizontal sample stacks with reflective insulations. Results showed that the predicted heat fluxes on the same area and same location of Heat Flux Transducers (HFTs) on the top and bottom surfaces of the sample stacks are in good agreement with the measured heat fluxes (within ±1%). The derived R-values using these heat fluxes are also in good agreements. Due to the combined effect of heat transfer by convection and radiation in the airspace (facing the reflective surface), these predicted and measured heat fluxes are greater than the area-weighted average heat flux of whole sample stack, which is needed to determine the effective R-value of the sample. As such, the derived R-value from the test data resulted in underestimation of the effective R-value of the sample stack. After gaining confidence in the present model, it was used to conduct parametric study in order to quantify the contribution of reflective insulations to the effective R-value for a sample stack with different inclination angles, different directions of heat flow (upward and downward) and for a wide range of foil emissivity. Furthermore, the present model was used to compare the predicted R-values with the listed R-values in the 2009 ASHRAE Handbook [22] for enclosed air cavity (20 mm thick) of different effective emittance, inclinations and directions of heat flow.

---

[*] Corresponding author, hamed.saber@nrc-cnrc.gc.ca, Phone: 613-993-9772

# Introduction

Global warming is one of the problems that we currently face. Designing roofing and wall systems of building envelope with potential energy savings and low risk of moisture related problems can help reduce the energy demand or loads for operating buildings, thereby reducing operating costs and contributing to the fight against global warming [1, 2]. One of the means to reduce the operating costs is to limit the heat transmission through building envelope. In additional to reflective insulations, there are a number of thermal insulations that can be used in conjunction with reflective insulation assemblies in the building envelope (e.g. glass and mineral fibre, polyurethane foam boards and in-situ foamed products, expanded and extruded polystyrene, etc). According to the Reflective Insulation Manufacturers Association International (RIMA-I), reflective insulation is defined as "*thermal insulation consisting of one or more low-emittance surfaces, bounding one or more enclosed air spaces*" [3]. Currently, reflective thermal insulation is being used in home attics, and roofing and wall systems [4]. In this application, the reflective insulation has at least one reflective surface that faces an airspace. As will be shown in this study, enclosed airspace contributes to the overall thermal resistance (R-value) of a system whether or not a reflective surface is installed in the system, but the reflective surface augments the thermal resistance of that airspace.

Within an enclosed airspace, which is a transparent medium, there are three modes of heat transfer: conduction, convection and radiation (see [5 - 8] for more details). The contribution of the enclosed airspace in roofing or wall systems to the R-values depends on a number of parameters, namely:
  (a) The emissivity of all surfaces bounded the airspace.
  (b) Size and orientation of the airspace.
  (c) Direction of heat transfer through the airspace. The rate of heat transfer by convection within an enclosed airspace is highly dependent on the direction of heat flow across it. For example, the contribution of airspace to the thermal resistance of a system with downward heat flow is greater than that for a system with upward heat flow. This is due

to a system with downward heat flow results in a relatively stable stratification of air due to differences in air buoyancy.

(d) Temperatures of all surfaces of the airspace. These temperatures are mainly affected by both outdoor and indoor conditions, and the amount of conventional insulation used in series with the airspace.

Within opaque materials, no thermal radiation is transmitted through these materials. Any surface of these materials that faces a transparent medium (e.g. airspace) absorbs and emits long-wave thermal radiation (e.g. surfaces of wood furring and drywall in furred-airspace assembly [5, 6, 7 and 8]). The amount of radiative heat transfer of this surface depends on its temperature and emissivity. Most of construction materials have a surface emissivity of 0.9 (ASHRAE 2009 [9]).

The contribution of the reflective insulation on the thermal performance (R-values and energy savings) of above-grade, and above- and below-grade wall systems with Furred-Airspace Assembly (FAA) were investigated in a number of publications [5, 6, 7 and 8]. In these wall systems, low emissivity material such as foil was installed within a furred-airspace assembly. A parametric study was conducted in order to investigate the effect of low emissivity of foil laminated to XPS foam when used within a furred – airspace assembly [5]. In that study, furring strips made of spruce (19 mm x 38 mm) were installed horizontally. Since there were no vertical studs in the wall assembly, the 2D version of the present model was suitable for this study. The results showed that the modelled wall system with foil emissivity of 0.05 increased the effective R-value by ~10% in the case of the indoor and outdoor temperatures of +20$^{o}$C and -20$^{o}$C, respectively [5].

The 3D version of the present model was recently benchmarked against the experimental data of a full-scale above-grade wall system (8' x 8') consisting of 2"x6" wood frame construction with stud cavities filled with friction-fit glass fibre batt insulation and a foil bonded to wood fibreboard installed in a furred-airspace assembly (the foil was facing the airspace and the interior finishes). Test was conducted in the Guarded Hot Box (GHB) to determine the effective thermal resistance of this wall system [10]. This test was conducted in accordance with ASTM C-1363 "Standard Test Method for the Thermal Performance of Building Assemblies by Means of a Hot Box Apparatus" [11]. Results showed that the predicted R-value of this wall system was in good agreement with the measured R-value [6].

The present model was used to investigate the effect of outdoor and indoor conditions on the steady-state and transient thermal performance of a foundation wall system (including the above-grade and below-grade portions of the wall) having FAA that incorporates a low emissivity material (foil) [7 and 8]. The external layer of the foundation wall was poured-in-place concrete and the internal layer was gypsum board. In order to quantify the contribution of a FAA with foil bonded to EPS foam on the energy savings in foundation wall systems, reference walls were considered (identical to these foundation walls but without FAA). Walls with and without FAA were subjected to two different climate loads where the measurements of soil temperature (2 m away from the wall), outdoor temperature and indoor temperature were used. Results showed that at steady-state condition, the effective R-value of wall with FAA can vary by as much as ~3%, depending on the soil, outdoor and indoor temperatures through the year. Moreover, these wall configurations resulted in an energy savings of ~17% more than the same walls but without FAA [7 and 8].

Note that in the previous studies [5 - 8], the orientation of the enclosed airspace was vertical (e.g. airspaces in wall systems). As indicated earlier, the reflective insulations can also be used in home attics, and flat and sloped roofs in order to reduce the solar heat gain within buildings. In these types of applications, enclosed airspace would have a zero or non-zero slope with a horizontal surface (e.g. flat or sloped roofing systems). Recently, Craven and Garber-Slaght [4] tested a number of reflective insulation products at the Cold Climate Housing Research Center (CCHRC) to quantify the contribution of airspace to the R-value of an assembly. Two types of reflective insulations (referred to in this paper as Type-A and Type-B) were tested using the ASTM C-518 test method [12] to measure their R-values. The CCHRC used a FOX-314 heat flow meter [13] that accommodates product samples up to 12" in width and length, and thickness up to 4". The Type-A and Type-B samples were placed between the two horizontal plates of the heat flow meter, at a constant temperature difference between the upper and lower plates. The measured R-values of these products were in good agreement with the reported R-values by the manufactures. The measured R-values of 1" thick of Type-A and 1" thick of Type-B were 4.02 ft$^2$ hr $^o$F/BTU (0.7080 m$^2$ K/W) and 3.87 ft$^2$ hr $^o$F/BTU (0.6815 m$^2$ K/W), respectively; and the derived thermal conductivities of these insulations were 0.03588 W/(m K) and 0.03727 W/(m K), respectively [4]. In order to quantify the thermal resistance added to the samples by creating a reflective insulation component, Craven and Garber-Slaght [4] used the ASTM C-518 test method after allowing for airspace of 1" thick between the reflective insulation (Type-A and

4

Type-B) and gypsum board of ½" thick (see Figure 1), where the total thickness of the sample stacks was less than 4" [12]. Those tests were performed at an average temperature of 75$^{o}$F (23.9$^{o}$C), with upper and lower surface temperatures of 55$^{o}$F (12.8$^{o}$C) and 95$^{o}$F (35.0$^{o}$C), respectively (upward heat flow through the samples).

The ASTM C-518 test method is suitable for determining the thermal resistance of a specimen in the case of one-dimensional heat flow through it. In the case of testing a sample stack such as shown in Figure 1 using this test method, the heat transfer through it will be by conduction, convection and radiation. This represents a multidimensional heat transfer through the sample stack where the middle layer with air cavity acts as thermal bridge. The use of heat flow meter apparatus according to the ASTM C-518 test method when there are thermal bridges present in the sample may yield results that are unrepresentative of the assembly (see [12] for more details). Alternatively, the ASTM C-1363 test method using the GHB can be used to determine the effective thermal resistance of sample with thermal bridges [11]. The present model was benchmarked in previous studies against the experimental data that was obtained using the ASTM C-1363 test method in the case of full-scale wall assemblies (8 feet x 8 feet) with reflective insulation [6] and without reflective insulations [14, 15 and 16]. As the wall R-value is affected by the indoor and outdoor ambient temperatures and wind speed, the boundary conditions that were used to benchmark the present model were: (a) convective boundary with the measured indoor temperature and heat transfer coefficient on the interior surface, (b) convective boundary with the measured outdoor temperature and heat transfer coefficient on the exterior surface, and (c) adiabatic boundary condition on the other surfaces of the wall assembly (i.e. no heat transfer). The predicted R-values were in good agreement with the measured R-values (see [6, 14, 15 and 16].

According to the ASTM C-518 test method [12], the thermocouples embedded in the surfaces of the upper and lower plates of the heat flow meter measure the temperature drop across the specimen and the Heat Flux Transducer (HFT) embedded in each plate measures the heat flow through the specimen. The uncertainty of the measurements in this test method is ±2%. Testing a sample using this method only requires preparing the sample and installing it between the hot and cold plates (i.e. no need to instrument the sample itself). As such, this test method sounds simple, accurate and a cost effective test. However, the question is "can the ASTM C-518 test method still be used to measure the effective thermal resistance of sample stack such as shown in Figure 1?". One of the objectives of this study is to answer this question. As

indicated earlier, the reflective insulations can be used in the roofing systems. In this type of applications, the reflective insulation would have a zero or non-zero slope with a horizontal surface. So, the other objective of this study is to quantify the contribution of reflective insulation to the R-value of sample stack with different inclination angles – the focus of the parametric study reported in this paper. Also, consideration is given to cover a wide range of the surface emissivity of the reflective insulation, and different directions of heat flow through the sample.

The NRC-IRC's hygrothermal model "hygIRC-C" was in this study to investigate the contribution of the reflective insulation to the R-value of specimens. This model solves simultaneously the 2D and 3D moisture transport equation, the energy equation, surface-to-surface radiation equation (e.g. surface-to-surface radiation in enclosed airspace such as shown in Figure 1) and the air transport equation in the various material layers. The air transport equation is the Navier-Stokes equation for the airspace (e.g. air cavity), and Darcy equation (Darcy Number, DN $<10^{-6}$) and Brinkman equation (DN $> 10^{-6}$) for the porous material layers. The present model was benchmarked [17] against the hygIRC-2D model that was previously developed at NRC-IRC [18, 19], and test results of different wall systems in a number of projects. The full descriptions of the present model are available elsewhere (e.g. see the references [1-2, 5-8, 15-17]).

# Comparison of Reported Test Data [4] and Present Model Predictions

The performance of reflective insulation depends on the emissivity of the foil bonded to the insulation and facing the airspace. This emissivity can increase due to: (a) oxidation of the foil, and accumulation of dust and/or vapor condensation on the surface of the foil. For example, Cook et al. [20] conducted experiments to investigate the effect of accumulation of dust on the emissivity on horizontal foil faces. That study showed that the emissivity of foil faces increases significantly as dust accumulates from an initial value of under 0.05 to an apparent asymptote ranging from 0.67 to 0.85, depending on the type of dust. Since most building materials have an emissivity of approximately 0.9 [9], the emissivity of all surfaces of different materials except the foil was taken equal to 0.9 in the numerical simulations. In order to quantify the effect of foil emissivity on the thermal performance and account for the possibility of dust and/or vapor

condensation on it, a range of foil emissivity of 0.0 – 0.9 was considered. Note that a foil emissivity of 0.9 represents the case of no foil installed in the system or the foil surface is completely covered by dust or liquid water due to condensation. Also, a foil emissivity of zero means that no thermal radiation is emitted from the surface (i.e. purely reflective surface).

The present model, hygIRC-C, was used to predict the effective thermal resistance of the sample stacks that were tested using the ASTM C-518 test method. Figure 1 shows the boundary conditions used in the numerical simulations. As shown in this figure, the top and bottom surfaces of the sample stacks were subjected to temperature boundary condition (55$^o$F (12.8$^o$C) for the top surface and 95$^o$F (35.0$^o$C) for the bottom surface). The side surfaces of these samples were subjected to adiabatic boundary conditions (i.e. no heat transfer). The measured thermal conductivities of the reflective insulations, Type-A and Type-B (0.03588 W/(m K) and 0.03727 W/(m K), respectively [4]) were used in the numerical simulations. Note that all results presented in this paper for the R-values are based on the surface-to-surface R-values (R-value = $\Delta T/q$”, where $\Delta T$ is the temperature difference between the hot and cold surfaces, and q” is the heat flux passing the specimen). Figure 2a, b and c show the predicted R-value of sample stack with different types of reflective insulations (2” thick of Type-A, see Figure 1b, and 1” thick of Type-A and 1” thick of Type-B, see Figure 1a) for a wide range of foil emissivity of 0.0 – 0.9. As shown in these figures, the predicted R-value decreases as the foil emissivity increases. For stack samples with 2” thick and 1” thick of Type-A, the predicted R-values decreases by 8.8% and 14.6%, respectively, as the foil emissivity increases from 0.05 to 0.9 (Figure 2a and b). Furthermore, for sample stack with 1” thick of Type-B, the predicted R-value decreases by 14.9% as the foil emissivity increases from 0.05 to 0.9 (Figure 2c).

As indicated earlier, Craven and Garber-Slaght [4] measured the R-value of these sample stacks in accordance of ASTM C-518 [12] using FOX-314 heat flow meter [13]. In that study, the emissivity of the foil bonded to the insulation of Type-A and Type-B were not measured. However, the authors stated that for shiny metal surfaces, the emissivity is around 0.05 – 0.1 according to ASHRAE (2009) [9]. The measured R-values of these sample stacks are compared with the predicted R-values in Figure 2 when the emissivity of these reflective insulations was assumed between 0.05 – 0.1.

The present prediction of the R-value of the sample stack with 2” thick of Type-A was 8.0% and 6.9% higher than the measured R-value for foil emissivity of 0.05 and 0.1, respectively (Figure

2a and Figure 3a). For sample stack with 1" thick of Type-A, the predicted R-value was also 8.5% and 6.8% higher than the measured R-value for foil emissivity of 0.05 and 0.1, respectively (Figure 2b and Figure 3b). Additionally, for sample stack with 1" thick of Type-B, the predicted R-value was 9.1% and 7.3% higher than the measured R-value for foil emissivity of 0.05 and 0.1, respectively (Figure 2c and Figure 3c). It is surprising that the present prediction of the R-value is consistently higher than the measured R-value (in accordance of ASTM C-518 test method [12] using FOX-314 heat flow meter [13]) by approximately the same percentage for different reflective insulations. In a previous study [6], however, the prediction of the present model for R-value was in good agreement (within 1.2%) with the measured R-value in GHB (in accordance of ASTM C-1363 test method [11]) for a full-scale wall system (8' x 8') having a reflective insulation and furred-airspace assembly. So, the question is "why was the predicted R-value found to be consistently higher than the measured R-value by approximately the same percentage for different reflective insulations using the ASTM C-518 test method with FOX-314 heat flow meter?"

It is expected that the combined effect of heat transfer by convection and radiation in the air cavity would result in higher heat fluxes on the middle portion of the top and bottom surfaces of the sample stacks where the Heat Flux Transducers (HFTs) were located. Thus, the measured heat fluxes may not represent the actual heat passing through the whole sample stack since these measurements would depend on the size of HFTs (4" x 4" in the FOX-314 heat flow meter [13]). Depending on the shape of heat flux distribution on the top and bottom surface (12" x 12"), using the measured heat fluxes to derive the R-value may result in determining lower R-value. Neither the measurements of heat fluxes were reported nor were the emissivity of the reflective surfaces measured [4]. So, it is hard to draw a conclusion at this moment about determining which R-value (predicted using the present model or derived from the test data) should be used to represent the effective R-value of sample stack with reflective insulations. To address these issues, a number of tests was conducted at NRC [21] using the ASTM C-518 test method as briefly described next.

## Tests Conducted at NRC [21]

This section summarizes the important findings obtained from the tests conducted at NRC in an attempt to answer the question raised above. However, the full descriptions of these tests are available in reference [21]. The tests were conducted in accordance of ASTM C-518 test

method [12] to measure the R-values of two sample stacks with and without aluminum foil. A heat flow meter that accommodates samples up to 12" in width and length, and thickness up to 4" was used. As shown in Figure 4, the sample stack consisted of upper and lower EPS layers; each has a size of 12 inch x 12 inch x 1 inch. To quantify the thermal resistance added to the samples by creating a reflective insulation component and determine the contribution to the R-value due to installing foil in the specimen, an air cavity (8 inch x 8 inch x 1 inch, same size as in reference [4]) was created in the center of another EPS layer (12 inch x 12 inch x 1 inch), which was placed between the upper and lower EPS layers. The first test was conducted without installing foil in the specimen. The second test was conducted after installing an aluminum foil on the bottom surface of the upper EPS layer (i.e. foil facing the airspace, see Figure 4). The emissivity of the aluminum foil was measured and found to be 0.2. Before conducting these two tests, the thermal conductivity of EPS layer was measured using the same test method (ASTM C-518) and the same heat flow meter. The measured thermal conductivity of three EPS samples were 0.03455, 0.03467 and 0.03470 W/(mK) with an average value of 0.03464 W/(mK). The value of the average thermal conductivity was used in the numerical simulations. The test results showed that the measured R-value in the case with aluminum foil ($\varepsilon = 0.2$) was 9.814 ft$^2$ hr $^o$F/BTU (within a standard deviation of ±1.07%). Also, the measured R-value in the case without aluminum foil ($\varepsilon = 0.9$) was 9.112 ft$^2$ hr $^o$F/BTU (within a standard deviation of ±0.86%) (see [21] for more details).

Figure 5 shows a comparison between the predicted R-value for different values of foil emissivity ranging from 0.0 to 0.9, and measured R-value for the cases with foil ($\varepsilon = 0.2$) and without foil ($\varepsilon = 0.9$). As shown in this figure, the predicted R-value decreases by 8.2% as the foil emissivity increases from 0.05 (R = 10.819 ft$^2$ hr $^o$F/BTU) to 0.9 (R = 9.999 ft$^2$ hr $^o$F/BTU). This reduction in R-value is approximately the same as the case of sample stack with 2" thick of Type-A (see [4]) shown in Figure 1b. Figure 5a and b show that the predicted R-values for the two cases of sample stacks with and without foil were 7.5% and 9.7%, respectively, higher than the measured R-values. Accordingly, the present model consistently predicts a higher R-values than the measured R-values by approximately the same percentage not only for the tests conducted at CCHRC but also for the tests conducted at NRC. Further investigations were needed to understand why the predicted R-value was consistently higher than the measured R-value, and which R-value would represent the effective R-value of the sample stacks. In these investigations, data analyses and a number of comparisons between the model predictions and measurements were carried out as presented next.

Since the measured temperatures at the interfaces between the sample stacks and the upper cold plate (12.7°C) and the lower hot plate (35.1°C) of the heat flow meter were taken as temperature boundary conditions in the numerical simulations, an accurate model should be able to predict the measured heat fluxes at these interfaces.  The predicted temperature distribution within the whole sample stack is shown in Figure 6a and b for $\varepsilon$ = 0.2 (aluminum foil) and $\varepsilon$ = 0.9 (no foil), respectively.  Also, Figure 7a and b show the velocity streamlines, and vertical velocity (v), horizontal velocity (u) and temperature distributions (T) in the air cavity of sample stacks with and without foil.  Owing to the temperature differential across the air cavity, a buoyancy-driven flow develops within it.  A multi-cellular airflow with six vortex cells is developed in the air cavity (see Figure 7 (a1) and (b1)).

A foil with lower emissivity has two interactive and competing effects on the different modes of heat transfer in the air cavity and hence on the effective R-value of the sample stack, namely:

(i)    A higher temperature gradient across the air cavity due to lower net radiative heat flux on the surfaces bounded the air cavity (see Figure 7 (a4) and (b4) for the cases with and without foil).  This effect results in an increase in the R-value for the case with lower emissivity.

(ii)    Stronger convection currents in the air cavity due to higher temperature gradient across it.  For example, the highest upward and downward velocities in the case with foil were 16.2 mm/s and 17.5 mm/s (Figure 7 (a2), which are greater than that in the case with without foil (9.6 mm/s and 10.1 mm/s, respectively, Figure 7 (b2)).  Furthermore, the highest horizontal velocity in the case with foil was 19.5 mm/s (Figure 7 (a3)) compared to 12.0 mm/s in the case without foil (Figure 7 (b3)).  This effect results in a decrease in the R-value for the case with lower emissivity.

The former effect was found to outweigh the latter effect, resulting in a higher effective R-value for a sample stack in the case with low foil emissivity than that in the case with high foil emissivity (e.g. see Figure 5).

The two interactive and competing effects described above result in non-uniform heat flux distributions on both the top and the bottom surfaces of the sample stack where the Heat Flux Transducers (HFTs) are located.  The size of the HFTs of the heat flow meter used in the tests conducted at NRC is 6 inch x 6 inch (152 mm x 152 mm), which are installed at the centers of the upper and lower plates.  Figure 8a and b show the predicted local heat fluxes at the top and

10

bottom surfaces of the sample stacks in the cases with and without foil, respectively. As shown in these figures, the convection loops (6 loops, see Figure 7) due to the multi-cellular airflow in the cavity resulted in higher heat fluxes on the middle portions of the top and bottom surfaces than that close to the edges. In the case with foil, the percentages of the maximum change in the heat fluxes on the top and bottom surfaces, respectively, are about 25% and 33% (Figure 8a). These percentages are 36% and 37% in the case without foil (Figure 8b). However, in order to use the ASTM C-518 test method [12], these percentages have to be ~0% (i.e. uniform heat flux distribution on the top and bottom surfaces (i.e. one-dimensional heat flow through the sample stack).

Consequently, it is obvious that with HFTs installed at the center of top and bottom surfaces having smaller size than the size of these surfaces results in measuring higher heat fluxes. Due to the non-uniformity of the heat fluxes on these surfaces, the measured heat fluxes are not representative to the actual heat passing through the whole sample stack. In this case, using the measured heat fluxes to drive the experimental R-value (R = $\Delta T/q''$, $\Delta T$ was controlled to be constant in the tests) would result in underestimation for the effective R-value. Since, the effective R-value has to be estimated based on the actual heat passing through the whole sample stack (or average heat flux based on area-weighted of whole surface of the sample stack), the predicted effective R-value is higher than the derived R-value using the measured heat flux. The author are therefore proposing that the phenomenon of non-uniformity of heat flux in the test apparatus, in combination with the smaller size of HFTs are the probable explanations for the predicted effective R-value being consistently higher than the derived R-value from the tests that were conducted at both NRC [21] and CCHRC [4].

## Benchmarking the Present Model

In order to show the non-uniformity of the predicted heat fluxes at the top and bottom surfaces of the sample stacks with and without foil, Table 1 lists the maximum, minimum and the area-weighted average heat fluxes based on whole surface area of 12" x 12" ($\overline{q}_{12x12}$). For the purpose of benchmarking the present model by comparing its predictions against the measurements, this table also lists the predicted area-weighted average heat fluxes at the middle of the sample stack on surface area of 6" x 6" ($\overline{q}_{6x6}$) and the measured values using HFTs of the same surface area. The standard deviation (STDEV) in all measurements of heat

fluxes was less than 2% [21]. As shown in Table 1, all measured and predicted $\overline{q}_{6\text{x}6}$ on the top and bottom surfaces of the sample stacks with and without foil are in good agreement (within $\leq$ $\pm1.0\%$).

As indicated earlier, the effective R-value for the sample stack should be obtained based on the actual heat passing through the specimen or $\overline{q}_{12\text{x}12}$. Just for the purpose of comparison, the predicted $\overline{q}_{6\text{x}6}$ and the measured heat fluxes were used to derive the R-value and compare it with the effective R-value (i.e. based on $\overline{q}_{12\text{x}12}$). Since the predicted $\overline{q}_{6\text{x}6}$ and the measured heat fluxes on the top and bottom surfaces are not equal (see Table 1 and Figure 9a), the mean value of the heat fluxes on both the top and bottom surfaces ($\overline{q}_{6\text{x}6,\text{mean}}$) were used to derive the R-values. The obtained results are plotted in Figure 9b. As shown in this figure, the derived R-values based on the predicted $\overline{q}_{6\text{x}6,\text{mean}}$ and the mean measured heat fluxes using 6"x6" HFTs are in good agreement (within $\pm0.6\%$) for the sample stacks with and without foil.

Using heat flow meter in accordance of the ASTM C-518 test method with HFTs that are smaller than the sample stack size (6" x 6" for the NRC's heat flow meter and 4" x 4" for the CCHRC's FOX-314 heat flow meter [4 and 13]) resulted in underestimation for the effective R-value. Depending on the value of the foil emissivity, the derived R-value from the test data underestimated the effective R-value by 7.5% and 9.7% for the cases with foil ($\varepsilon = 0.2$) and without foil ($\varepsilon = 0.9$), respectively (see Figure 9b).

In summary, based on the results presented above, measuring the effective R-value of sample stacks with reflective insulations such as presented in this study by using the ASTM C-518 test method [12] is not recommend with a heat flow meter that has HFTs with surface area less than the surface area of top and bottom surfaces of the specimen. Because the ASTM C-518 test method is quite simple, accurate (uncertainty of the measurement is within 2% [12]), and cost effective, it is worth trying to test the applicability of this method with a heat flow meter when the surface areas of the HFTs and the top and bottom surfaces of the specimen are equal. After gaining confidence in the present model, it was used to investigate the effect of the inclination angle and direction of heat flow of sample stack with reflective insulation on its thermal performance as shown next.

# Effect of Inclination Angle and Direction of Heat Flow

As indicated earlier, the reflective insulations are being used in sloped roof systems. In this particular application, it might be difficult to adapt one of the available test methods (ASTM C-518, ASTM C-1363) in order to measure the R-value of specimen with reflective insulation. For instance, the ASTM C-518 test method could be used in the case of specimen with horizontal and vertical orientations only [12]. After gaining confidence in the present model in predicting the R-value of specimen with horizontal orientation (see the pervious section) and specimen with vertical orientation (e.g. see [6]), it was used to quantify the contribution of reflective insulation to the R-value of specimen with different orientations.

In this section, a parametric study was conducted to investigate the effect of inclination angle ($\theta$), foil emissivity ($\varepsilon$), and direction of heat flow on the effective R-value of EPS sample stack shown in Figure 4. Note that the rate of heat transfer by both convection and radiation in the air cavity depends on its size and the temperature difference across the sample stack ($\Delta T$). As such, the effective R-value depends on both $\Delta T$ and the size of the air cavity. The results presented in this section are obtained for *only* one $\Delta T = 22.4^{\circ}C$ ($T_c = 12.7^{\circ}C$, and $T_h = 35.1^{\circ}C$) and one size of the air cavity.

In the case of foil emissivity of 0.05, Figure 10 and Figure 11 show the vertical velocity (v) and horizontal velocity (u) contours and the airflow field in the cavity for different $\theta$ when the sample stack was heated from the top and the bottom. As shown in these figures, in the case of sample stack heated from the top with $\theta = 30^{\circ}$ and vertical sample stack heated from the left ($\theta = 90^{\circ}$), a mono-cellular with one vortex cell airflow is developed in the air cavity. In the case of sample stack heated from the bottom with $\theta = 30^{\circ}$, a multi-cellular airflow is developed in the cavity with three vortex cells. For horizontal sample stack ($\theta = 0^{\circ}$) heated from the bottom and top, multi-cellular airflow is developed in the cavity with six and two vortex cells, respectively.

Figure 10 and Figure 11 show that the value of the air velocity in the cavity is greatly affected by both $\theta$ and direction of heat flow through the sample stack. For horizontal sample stack ($\theta = 0^{\circ}$), the air velocity in the case of downward heat flow (sample heated from the top, $v\uparrow(max) = 0.6$ mm/s, $u\rightarrow (max) = 3.2$ mm/s, Table 2) is much smaller than that in the case of upward heat flow (sample heated from the bottom, $v\uparrow(max) = 18.7$ mm/s, $u\rightarrow (max) = 22.1$ mm/s, Table 2). This

is due to a downward heat flow encourages a relatively stable stratification of air due to differences in buoyancy compared to the case with upward heat flow. As such, a sample stack with downward heat flow results in a grater R-value (12.19 ft$^2$hr$^o$F/BTU) than that with upward heat flow (10.82 ft$^2$hr$^o$F/BTU) (see Figure 12a). By subtracting the R-value of both the top and bottom EPS layers (8.33 ft$^2$hr$^o$F/BTU) from the total R-value of the sample stack, the middle layer with the air cavity contributed to the R-value by 3.86 ft$^2$hr$^o$F/BTU and by 2.49 ft$^2$hr$^o$F/BTU in the case of horizontal sample stack heated from the top and bottom, respectively (Figure 12b). Similarly, for $\theta = 30^o$, the air velocity in the cavity of sample stack heated from the top (v↑(max) = 10.6 mm/s, u→ (max) = 18.5 mm/s, Table 2) is also smaller than that heated from the bottom (v↑(max) = 14.1 mm/s, u→ (max) = 23.3 mm/s, Table 2). Consequently, the contribution of middle layer with air cavity to the R-value for the former (3.26 ft$^2$hr$^o$F/BTU) is greater than that for the latter (2.65 ft$^2$hr$^o$F/BTU) (Figure 12b). For vertical sample stack ($\theta = 90^o$) heated from the left or right, the contribution of the middle layer with air cavity to the R-value is 2.63 ft$^2$hr$^o$F/BTU.

Figure 13a and Figure 13b show the effect of the foil emissivity on the effective R-value and the contribution of the middle layer with air cavity to the R-value, respectively, for sample stack with different inclination angles and different directions of heat flow. As shown in these figures, for all values of foil emissivity, the horizontal sample stack heated from the top (downward heat flow) resulted in the highest R-values while the horizontal sample stack heated from the bottom (upward heat flow) resulted in the lowest R-values. These two cases, respectively, represent the application of using reflective insulations in flat roof in the summer season and winter season. As indicated earlier, the foil emissivity can increase due to oxidation of the foil, accumulation of dust (see [20]) and/or vapor condensation on the surface of the foil. Increasing the foil emissivity from 0.05 to 0.9 resulted in a decrease in the R-value by 20.7% and 8.2% for horizontal sample stack heated from the top and bottom, respectively (Figure 13a). Note that the emissivity of 0.9 represents the case of no foil installed on the system. Moreover, as the foil emissivity increases from 0.05 to 0.9, the contribution of the air cavity to the R-value decreases by 118% (from 3.86 ft$^2$hr$^o$F/BTU to 1.77 ft$^2$hr$^o$F/BTU) and 49% (from 2.49 ft$^2$hr$^o$F/BTU to 1.67 ft$^2$hr$^o$F/BTU) for horizontal sample stack heated from the top and bottom, respectively (Figure 13b).

In the case of sample stack with inclination angle of 30$^o$ (e.g. application of reflective insulations in sloped roof), increasing the foil emissivity from 0.05 to 0.9 resulted in a decrease in the R-

value by 15.0% and 9.5% for sample stack heated from the top (summer season) and bottom (winter season), respectively (Figure 13a). Also, Figure 13b shows that as the foil emissivity increases from 0.05 to 0.9, the contribution of the air cavity to the R-value decreases 86% (from 3.26 ft$^2$hr$^o$F/BTU to 1.75 ft$^2$hr$^o$F/BTU) and 56% (from 2.65 ft$^2$hr$^o$F/BTU to 1.70 ft$^2$hr$^o$F/BTU) for sample stack heated from the top and bottom, respectively. Furthermore, in the case of vertical sample stack (e.g. application of reflective insulations in wall systems), increasing the foil emissivity from 0.05 to 0.9 resulted in a decrease in the R-value by 11.0% (Figure 13a). In this case the contribution of the air cavity to the R-value decreases by 68% (from 2.81 ft$^2$hr$^o$F/BTU to 1.67 ft$^2$hr$^o$F/BTU).

In the case of no foil installed in sample stack or the foil surface is fully covered by dust and/or vapor condensation (i.e. $\varepsilon$ = 0.9), both inclination angle and direction of heat flow through the specimen have insignificant effect on the effective R-value (i.e. resultant lines tend to converge as $\varepsilon$ tends to 0.9, see Figure 13a). In this case, the maximum change in the contribution of air cavity to the R-value is only 6% (from 1.77 ft$^2$hr$^o$F/BTU to 1.67 ft$^2$hr$^o$F/BTU, Figure 13b). Therefore, for accurate energy calculations for roof and wall systems with reflective insulations, subjected to different climate conditions, it is important to conduct hygrothermal simulations instead of thermal simulations in order to investigate whether or not vapor condensation occurs on the surface of the foil.

Note that the results in Figure 12b and Figure 13b presented the contribution of the middle EPS layer with the air cavity (1" thick) to the effective R-value of sample stack with reflective insulations. The 2009 ASHRAE Handbook [22] lists the R-values of only plane air cavities for different combined or effective emittance of the cavity's hot and cold faces. Finally, the present model was used to compare the predicted R-values with that listed in ASHRAE Handbook. The obtained results are presented next.

## Comparison between the Predicted R-values with the Listed R-Values in ASHRAE Handbook

A table in the 2009 ASHRAE Handbook, chapter 26 [22] listed the R-values for enclosed air cavities for various conditions, depending on the combined or effective emittance ($\varepsilon_{eff}$) of the

cavity's hot and cold surfaces. The effective emittance is defined as: $1/\varepsilon_{eff} = 1/\varepsilon_1 + 1/\varepsilon_2 - 1$,

where $\varepsilon_1$ and $\varepsilon_2$ are the emissivity of the hot and cold surfaces. That table provided the R-values of enclosed air cavities of four thicknesses (13, 20, 40 and 90 mm), and subjected to four mean temperatures $T_{mean}$, (32.2, 10.0, -17.8, -45.6$^o$C) and three temperature differences, $\Delta T$, (5.6, 11.1, 16.7$^o$C) [22]. As indicated earlier, the present model was benchmarked in the case of enclosed air cavity of 1 inch (25.4 mm) thick, and the closest thickness of the air cavity in ASHRAE table was 20 mm. As such, numerical simulations were conducted in order to compare the present prediction of R-value with that listed in ASHRAE table for enclosed air cavity of 20 mm thick.

Since the length of the enclosed air cavity is not specified in the ASHRAE table, and it is needed to define the computational domain, a sensitivity analysis was conducted to investigate its effect on the R-value. Three cavity lengths were considered in this analysis: 4" (101.6 mm), 8" (203.2 mm) (same as the case considered earlier) and 16" (406.4 mm). For $\varepsilon_{eff}$ = 0.05, $T_{mean}$ = 32.2$^o$C, $\Delta T$ = 5.6$^o$C, Table 3 compares the predicted and ASHRAE R-values for horizontal air cavity with different lengths in the case of upward heat flow. As shown in this table, the cavity length has some effect on its R-value. For example, increasing the cavity length from 4" to 8" and from 4" to 16" resulted in an increase in its R-value by 1.5% and 3.7%, respectively. Also, increasing the cavity length form 8" to 16" resulted in an increase in the R-value by 2.1%. Table 3 shows that the ASHRAE R-value was 14.8%, 13.0% and 10.7% higher than the predicted R-value for the cavity length of 4", 8" and 16", respectively.

In the case of upward heat flow in a horizontal cavity (8" long), Figure 14 and the first row in Table 4 (Case I) compare the predicted and ASHRAE R-values for different effective emittance at $T_{mean}$ = 32.2$^o$C, $\Delta T$ = 5.6$^o$C. As shown in the figure, both the predicted and ASHRAE R-values are in good agreements (within $\leq \pm$3.5%) for the case of high $\varepsilon_{eff}$ (0.5 and 0.82). For low effective emittance, however, the ASHRAE R-value is 14.0%, 13.0% and 6.1% higher than the predicted R-value for $\varepsilon_{eff}$ = 0.03, 0.05 and 0.2, respectively. This finding at low emissivity is in agreement with a recent study by Craven and Garber-Slaght [4]. In that study, it was shown that the ASHRAE R-value [22] was also higher than the measured R-value in the case with low emissivity.

To compare the predicted and ASHRAE R-values in the case of different inclination angles, directions of heat flow, and effective emittance, numerical simulations were conducted for enclosed air cavity (20 mm thick, 8" long) when it was subjected to $T_{mean} = 32.2^oC$, $\Delta T = 5.6^oC$ for the following five cases:

- Case I: horizontal cavity ($\theta = 0^o$) with upward heat flow (Figure 15a),
- Case II: inclined cavity ($\theta = 45^o$) with upward heat flow (Figure 15b),
- Case III: vertical cavity ($\theta = 90^o$) with horizontal heat flow (Figure 15c),
- Case IV: inclined cavity ($\theta = 45^o$) with downward heat flow (Figure 15d), and
- Case V: horizontal cavity ($\theta = 0^o$) with downward heat flow (Figure 15d).

The obtained results for the vertical velocity distribution and flow streamlines for these five cases are shown in Figure 15a - Figure 15e when $\varepsilon_{eff} = 0.03$.

Table 4 compares the predicted and ASHRAE R-values for the five cases described above. As shown in this table, the predicted and ASHRAE R-values are in good agreement for all values of $\varepsilon_{eff}$ (within $\leq \pm6.3\%$) for Case II (Figure 15b) and Case V (Figure 15e). For Case III (Figure 15c) and Case IV (Figure 15d), the predicted and ASHRAE R-values are in good agreement (within $\leq \pm2.0\%$) for high $\varepsilon_{eff}$ (0.5 and 0.82). For low $\varepsilon_{eff}$ in Case III, the ASHRAE R-values are 24.9%, 21.7% and 12.7% higher than the predicted R-value for $\varepsilon_{eff} = 0.03$, 0.05 and 0.2, respectively. Also, for low $\varepsilon_{eff}$ in Case IV, the ASHRAE R-values are 16.5%, 16.1% and 7.7% higher than the predicted R-value for $\varepsilon_{eff} = 0.03$, 0.05 and 0.2, respectively.

# Summary and Conclusions

Numerical simulations were conducted to address the thermal performance of different types of reflective insulations. The present model was used to explore the possibility of using the ASTM C-518 test method for measuring the effective R-value of sample stack with reflective insulations. In the first phase of this study, the predictions of the present model were compared with the CCHRC's test data that were obtained using FOX-314 heat flow meter in accordance of ASTM C-518 test method. Results showed that the predicted R-values were consistently 6.8 – 9.1% higher than the R-values derived from the test data [4]. To understand why the predicted R-values were consistently higher than the measured ones, two tests were conducted at NRC for EPS sample stack with and without aluminum foil using the same test method and same test

conditions as in reference [4] but with different heat flow meter. It was found that the predicted R-values were 7.5% and 9.7% higher than the R-values derived from the test data for the cases with and without foil. The full description of the tests conducted at NRC is available in [21].

Further investigations were needed to understand why the predicted R-value was consistently higher than the measured R-value at both CCHRC [4] and NRC [21], and which R-value would represent the effective R-value of the sample stacks. It was found that the predicted heat flux distributions were non-uniform on the top and bottom surfaces of the sample stack due to the combined effect of heat transfer by convection and radiation inside the air cavity. As a step for benchmarking the present model, the predicted heat fluxes on the same area and same location of Heat Flux Transducers (HFTs) on the top and bottom surfaces of the sample stacks were compared. Results showed that both predicted and measured heat fluxes as well as the derived R-values using these heat fluxes were in good agreement (within ±1%). Because these heat fluxes are not fully representative to the actual heat passing through the sample stack, the effective R-value (based on the area-weighted average heat flux of whole sample stack) is greater than that derived R-value from the test data. Based on the results presented in this study, it is not recommended to use heat flow meter in accordance of ASTM C-518 test method to measure the R-value of sample stacks with reflective insulations as this test method resulted in underestimation of the effective R-value. Since ASTM C-518 test method is quite simple, accurate (uncertainly within ±2%), and cost effective, future work is recommended to investigate the possibility of using this test method to accurately measure the effective R-value of sample stacks with reflective insulations after: (a) increasing the size of the HFTs to be the same as the size of the top and bottom surfaces of the sample stack, and/or (b) reducing the size of the top and bottom surface of the sample stack to be the same as the size of the HFTs.

After benchmarking the present model, it was used to quantify the contribution of reflective insulations to the effective R-value for a sample stack with different inclination angles, different directions of heat flow and for a wide range of foil emissivity. The results showed that increasing the foil emissivity from 0.05 to 0.9 resulted in a decrease in the effective R-value by 20.7% and 8.2% for horizontal sample stack heated from the top and bottom, respectively. For inclination angle of 30°, increasing the foil emissivity from 0.05 to 0.9 resulted in a decrease in the effective R-value by 15.0% and 9.5% for sample stack heated from the top and bottom, respectively. Furthermore, increasing the foil emissivity from 0.05 to 0.9 resulted in a decrease in the effective R-value by 11.0% for vertical sample stack.

Finally, this study was further expanded to compare the predicted R-values with that listed in the 2009 ASHRAE Handbook [22] of a plane air cavity (20 mm thick) and subjected to a mean temperature of 32.2$^o$C, and temperature difference of 5.6$^o$C for different: (a) effective emittance of the cavity's hot and cold faces, (b) inclination angles, and directions of heat flow. The obtained results were listed in Table 4. This work would be helpful for architects and building designers to quantify the contribution of the reflective insulation to the effective thermal resistance of specimens with different emissivities, inclination angles and environmental conditions in energy saving. A future work is recommended in order to cover different applications of the reflective insulations that use actual R-value of insulation under different climatic conditions so as to avoid over sizing the heating and cooling equipments and condensation risk.

# References

1. H.H. Saber, M.C. Swinton, P. Kalinger, and R.M. Paroli, "Hygrothermal Simulations of Cool Reflective and Conventional Roofs", 2011 NRCA International Roofing Symposium, Emerging Technologies and Roof System Performance, held in Sept. 7-9, 2011, Washington D.C., USA.

2. H.H. Saber, M.C. Swinton, P. Kalinger, and R.M. Paroli, "Long-Term Hygrothermal Performance of White and Black Roofs in North American Climates", Journal of Building and Environment, in press, October 2011.

3. Reflective Insulation Manufacturers Association International (RIMA-I). Reflective Insulation, Radiant Barriers and Radiation Control Coatings. Olathe, KS: RIMA-I, 2002.

4. C. Craven, and R. Garber-Slaght, "Product Test: Reflective Insulation in Cold Climates", Technical Report Number TR 2011-01, Cold Climate Housing Research Center (CCHRC), Fairbanks, AK 99708, www.cchrc.org, April 12, 2011.

5. H.H. Saber, and M.C. Swinton, "Determining through numerical modeling the effective thermal resistance of a foundation wall system with low emissivity material and furred – airspace", 2010 International Conference on Building Envelope Systems and Technologies, ICBEST 2010, Vancouver, British Colombia, Canada, June 27-30, 2010, pp. 247-257.

6. H.H. Saber, W. Maref, M.C. Swinton, and C. St-Onge, "Thermal analysis of above-grade wall assembly with low emissivity materials and furred-airspace," Journal of Building and

Environment, volume 46, issue 7, pp. 1403-1414, 2011 (doi:10.1016/j.buildenv.2011.01.009).

7. H.H. Saber, W. Maref and M.C. Swinton, "Numerical investigation of thermal response of basement wall systems with low emissivity material and furred – airspace", 13th Canadian Conference on Building Science and Technology (13th CCBST) Conference, held in May 10 – 13, 2011 in Winnipeg, Manitoba, Canada.

8. H.H. Saber, W. Maref, and M.C. Swinton, "Thermal Response of Basement Wall Systems with Low Emissivity Material and Furred Airspace", Journal of Building Physics, Published online in 5 August 2011, DOI: 10.1177/1744259111411652, The online version of this article can be found at: http://jen.sagepub.com/content/early/2011/07/30/1744259111411652.

9. ASHRAE (2005). Chapter 25. Thermal and Water Vapor Transmission Data. ASHRAE Handbook – Fundamentals. Atlanta, GA: American Society of Heating, Refrigeration and Air-Conditioning Engineers, Inc.

10. Air- Ins inc, Performance Evaluation of Enermax Product Tested For CCMC Evaluation Purposes as per CCMC Technical Guide Master Format 07 21 31.04, Confidential Test Report Prepared for Products of Canada Corp., AS-00202-C, August 17th, 2009.

11. ASTM. 2006. ASTM C-1363, Standard Test Method for the Thermal Performance of Building Assemblies by Means of a Hot Box Apparatus, 2006 Annual Book of ASTM Standards 04.06:717–59, www.astm.org.

12. ASTM. 2003, ASTM C-518, Standard Test Method for Steady-State Heat Flux Measurements and Thermal Transmission Properties by Means of the Heat Flow Meter Apparatus, Annual Book of Standards, 04.06, 153-164, American Society for Testing and Materials, Philadelphia, Pa, www.astm.org.

13. FOX-314 Heat Flow Meter, http://engrwww.usask.ca/script/beaverden/pubservice.php?htmlareaupload=2328&sh=01159ab2b5cbdcf4814d0d336fb462fc, Last visited in June 2011.

14. A.H. Elmahdy, W. Maref, M.C. Swinton, H.H. Saber, and R. Glazer, "Development of Energy Ratings for Insulated Wall Assemblies", 2009 Building Envelope Symposium (San Diego, CA. 2009-10-26) pp. 21-30, 2009.

15. H.H. Saber, W. Maref, A.H. Elmahdy, M.C. Swinton, and R. Glazer, "3D thermal model for predicting the thermal resistances of spray polyurethane foam wall assemblies", Building XI Conference, December 5-9, 2010, Clearwater Beach, Florida, USA.

16. H.H. Saber, W. Maref, H. Elmahdy, M.C. Swinton, and R. Glazer, "3D Heat and Air Transport Model for Predicting the Thermal Resistances of Insulated Wall Assemblies", International Journal of Building Performance Simulation, (http://dx.doi.org/10.1080/19401493.2010.532568), First published on: 24 January 2011 (iFirst), pp. 1-17.

17. H.H. Saber, W. Maref, M.A. Lacasse, M.C. Swinton, M.K. Kumaran, "Benchmarking of hygrothermal model against measurements of drying of full-scale wall assemblies", 2010 International Conference on Building Envelope Systems and Technologies, ICBEST 2010, Vancouver, British Colombia Canada, June 27-30, 2010, pp. 369-377.

18. W. Maref, M.K. Kumaran, M.A. Lacasse, M.C. Swinton, D. van Reenen, "Laboratory measurements and benchmarking of an advanced hygrothermal model", Proceedings of the 12th International Heat Transfer Conference (Grenoble, France, August 18, 2002), pp. 117-122, October 01, 2002 (NRCC-43054).

19. W. Maref, M.A. Lacasse, M.K. Kumaran, M.C. Swinton, "Benchmarking of the advanced hygrothermal model-hygIRC with mid-scale experiments", eSim 2002 Proceedings (University of Concordia, Montreal, September 12, 2002), pp. 171-176, October 01, 2002 (NRCC-43970).

20. J.C. Cook, D.W. Yarbrough, and K.E. Wilkes, "Contamination of Reflective Foils in Horizontal Applications and the Effect on Thermal Performance", ASHRAE Transactions, Vol. 95, Part 2, 677-381, 1989.

21. H.H. Saber, W. Maref, G. Sherrer, and M.C. Swinton, "Numerical Modelling and Experimental Investigations of Thermal Performance of Reflective Insulations", submitted to the Journal of Building Physics, October, 2011.

22. ASHRAE (2009). Chapter 26. Heat, Air, and Moisture Control in Building Assemblies – Material Properties. ASHRAE Handbook – Fundamentals. SI Edition, Atlanta, GA: American Society of Heating, Refrigeration and Air-Conditioning Engineers, Inc.

**Table 1.** Comparison of predicted and measured heat fluxes (in W/m$^2$) on the top and bottom surfaces of sample stacks with and without foil

| | Parameter | | | with foil ($\varepsilon$ = 0.2) | without foil ($\varepsilon$ = 0.9) |
|---|---|---|---|---|---|
| **Predicted** | Top surface | | max | 13.091 | 14.017 |
| | | | min | 10.512 | 10.338 |
| | | | avg on 12"x12" ($\overline{q}_{12x12}$) | 12.052* | 12.721* |
| | | | avg on 6" x 6" ($\overline{q}_{6x6}$) | 12.665 | 13.848 |
| | Bottom surface | | max | 13.314 | 14.016 |
| | | | min | 10.040 | 10.251 |
| | | | avg on 12"x12" ($\overline{q}_{12x12}$) | 12.052* | 12.721* |
| | | | avg on 6" x 6" ($\overline{q}_{6x6}$) | 13.069 | 13.898 |
| | Mean value on 6"x6" of both top and bottom surfaces ($\overline{q}_{6x6,mean}$) | | | 12.867 | 13.873 |
| **Measured using 6"x6" heat flux transducers (see [21] for more details)** | Top surface | | avg using 6"x6" HFT | 12.726 | 13.951 |
| | | | STDEV (W/m$^2$) | 0.118 | 0.104 |
| | | | STDEV (%) | 0.930 | 0.744 |
| | Bottom surface | | avg using 6"x6" HFT | 13.114 | 13.759 |
| | | | STDEV (W/m$^2$) | 0.249 | 0.215 |
| | | | STDEV (%) | 1.896 | 1.564 |
| | Mean value on 6"x6" of both top and bottom surfaces ($\overline{q}_{6x6,mean}$) | | | 12.920 | 13.855 |
| **Deviation from experiment (%)** | Top surface | | | 0.474 | 0.737 |
| | Bottom surface | | | 0.343 | -1.006 |
| | Mean value on 6"x6" of both top and bottom surfaces | | | 0.407 | -0.129 |

* The values on the top and bottom surfaces are equal due to energy conservation (see Figure 9a)

**Table 2.** Max vertical and horizontal air velocity in the air cavity of the sample stack inclination shown in Figure 4 with different inclination (T$_c$ = 12.7$^o$C, T$_h$ = 35.1$^o$C, $\varepsilon$ = 0.05)

| Sample stack | Inclination angles, $\theta$ ($^o$) | Max vertical velocity, v (mm/s) | | Max horizontal velocity, u (mm/s) | |
|---|---|---|---|---|---|
| | | v↑(max) | v↓(max) | u→(max) | u←(max) |
| **Heated from top** | 0$^o$ | 0.6 | -4.3 | 3.2 | -3.2 |
| **Heated from bottom** | 0$^o$ | 18.7 | -20.4 | 22.1 | -22.1 |
| **Heated from top** | 30$^o$ | 10.6 | -12.4 | 18.5 | -18.5 |
| **Heated from bottom** | 30$^o$ | 14.1 | -15.3 | 23.3 | -21.8 |
| **Heated from left** | 90$^o$ | 35.4 | -35.4 | 14.3 | -11.9 |

**Table 3.** Comparison between the predicted and ASHRAE R-values for horizontal enclosed air cavity (20 mm thick) with different lengths in the case of upward heat flow, $T_{mean} = 32.2^{\circ}C$, $\Delta T = 5.6^{\circ}C$, and $\varepsilon_{eff} = 0.05$[#]

| Cavity Length inch (mm) | R-value (m²K/W) Predicted | R-value (m²K/W) ASHRAE | Dev (%) |
|---|---|---|---|
| 4 (101.6) | 0.3399 | 0.3900 | 14.75 |
| 8 (203.2) | 0.3450 | 0.3900 | 13.03 |
| 16 (406.4) | 0.3523 | 0.3900 | 10.69 |

[#] $T_{mean}$ = mean temperature ($^{\circ}C$), $\Delta T$ = temperature difference ($^{\circ}C$), $\varepsilon_{eff}$ = effective emittance

**Table 4.** Comparison between the predicted and ASHRAE R-values for enclosed air cavity (20 mm thick and 8" (203.2) long) with different inclinations and direction of heat flow in the case of $T_{mean} = 32.2^{\circ}C$, $\Delta T = 5.6^{\circ}C$, and $\varepsilon_{eff} = 0.03$

| Case* | Effective Emissivity ($\varepsilon_{eff}$) | | | | | | | | | | | | | | |
|---|---|---|---|---|---|---|---|---|---|---|---|---|---|---|---|
| | 0.03 | | | 0.05 | | | 0.2 | | | 0.5 | | | 0.82 | | |
| | R-Value (m²K/W) | | Dev (%) | R-Value (m²K/W) | | Dev (%) | R-Value (m²K/W) | | Dev (%) | R-Value (m²K/W) | | Dev (%) | R-Value (m²K/W) | | Dev (%) |
| | Present | ASHRAE | | Present | ASHRAE | | Present | ASHRAE | | Present | ASHRAE | | Present | ASHRAE | |
| I | 0.3598 | 0.4100 | 13.95 | 0.3450 | 0.3900 | 13.03 | 0.2640 | 0.2800 | 6.08 | 0.1800 | 0.1800 | 0.01 | 0.1347 | 0.1300 | -3.52 |
| II | 0.5163 | 0.5200 | 0.71 | 0.4859 | 0.4900 | 0.84 | 0.3368 | 0.3300 | -2.02 | 0.2092 | 0.2000 | -4.40 | 0.1493 | 0.1400 | -6.25 |
| III | 0.4964 | 0.6200 | 24.90 | 0.4682 | 0.5700 | 21.74 | 0.3283 | 0.3700 | 12.71 | 0.2059 | 0.2100 | 1.99 | 0.1476 | 0.1500 | 1.61 |
| IV | 0.5321 | 0.6200 | 16.53 | 0.4998 | 0.5800 | 16.05 | 0.3435 | 0.3700 | 7.73 | 0.2117 | 0.2100 | -0.81 | 0.1506 | 0.1500 | -0.40 |
| V | 0.5863 | 0.6200 | 5.74 | 0.5473 | 0.5800 | 5.97 | 0.3649 | 0.3700 | 1.40 | 0.2195 | 0.2100 | -4.33 | 0.1544 | 0.1500 | -2.85 |

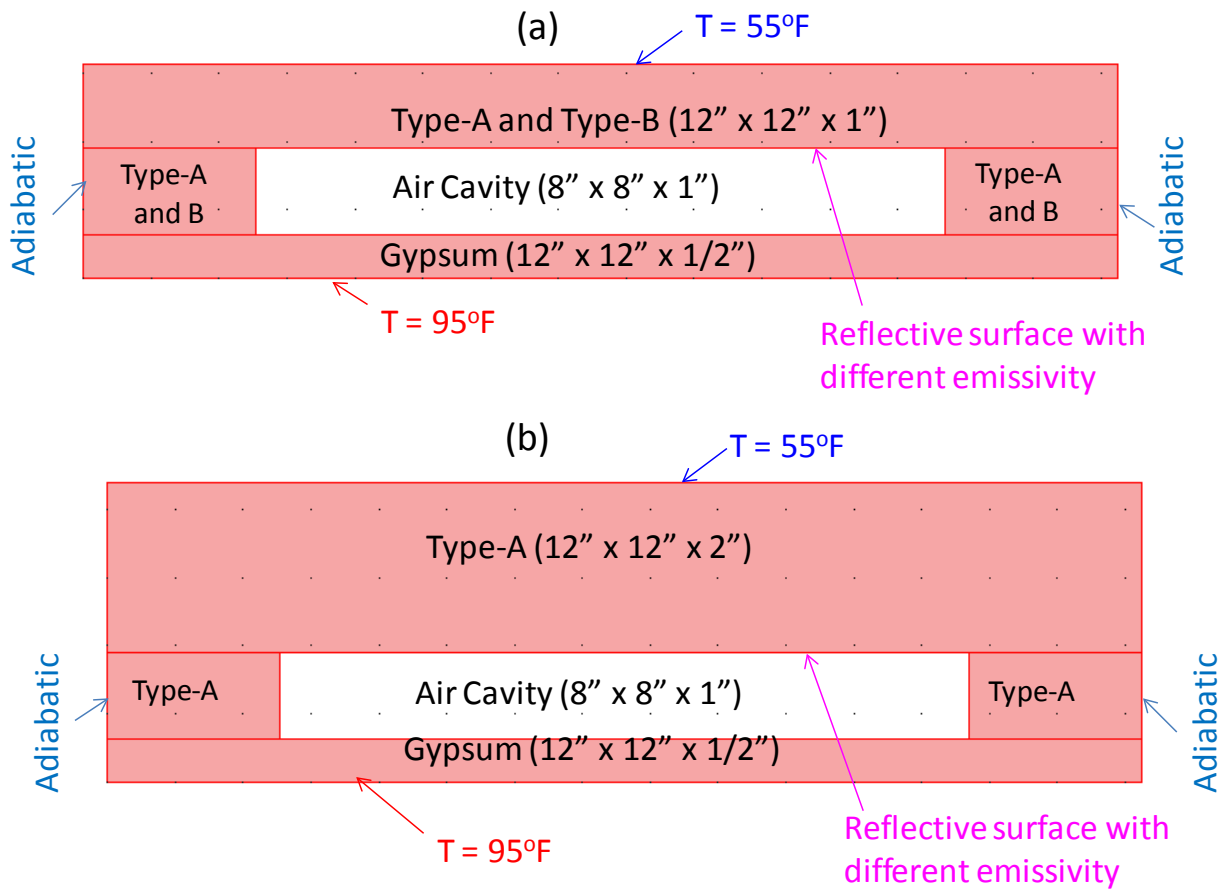* See Figure 15 for the case definition

**Figure 1.** Sample stack with reflective insulations (Type-A and Type-B) tested at CCHRC [4]
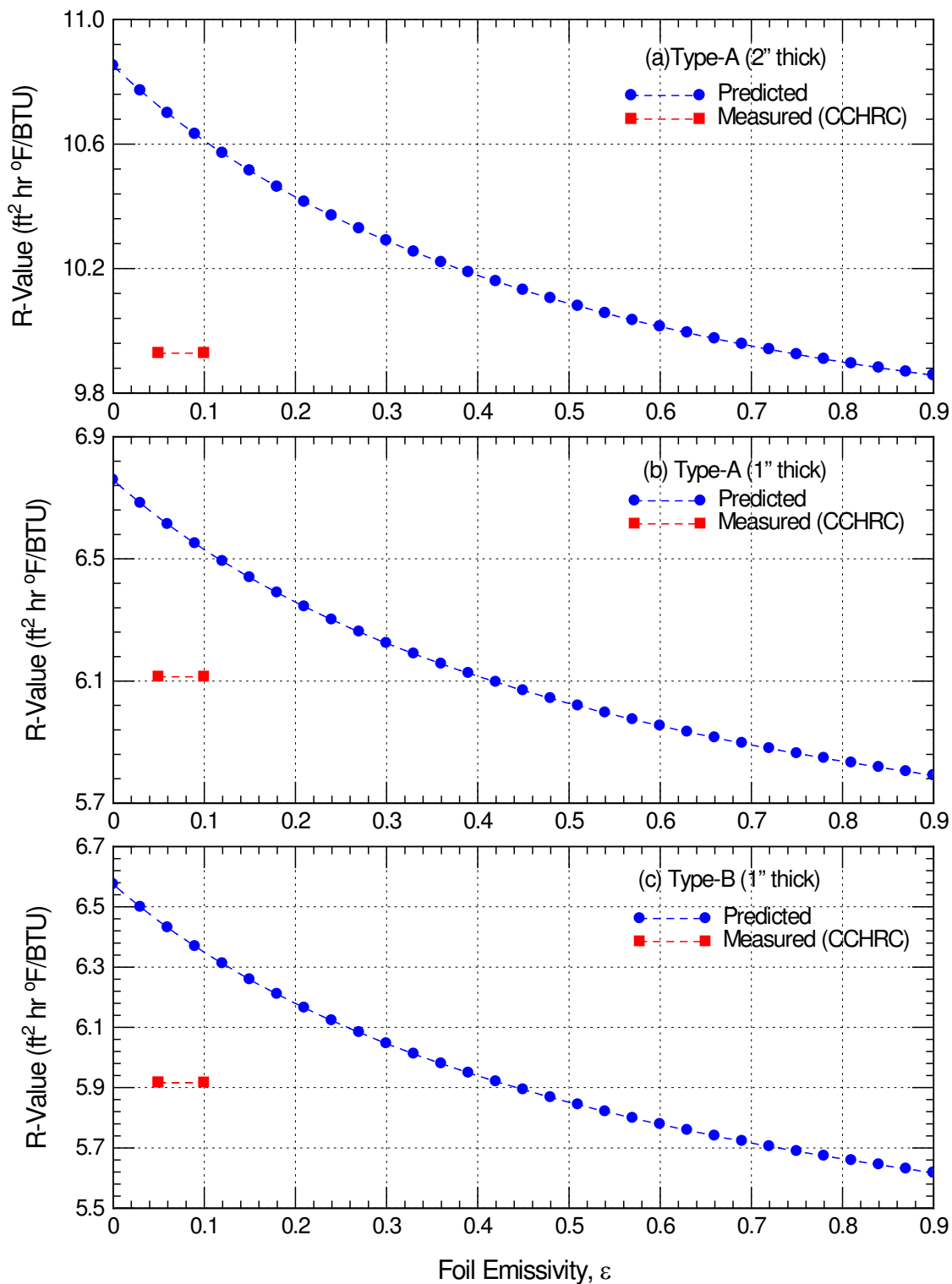
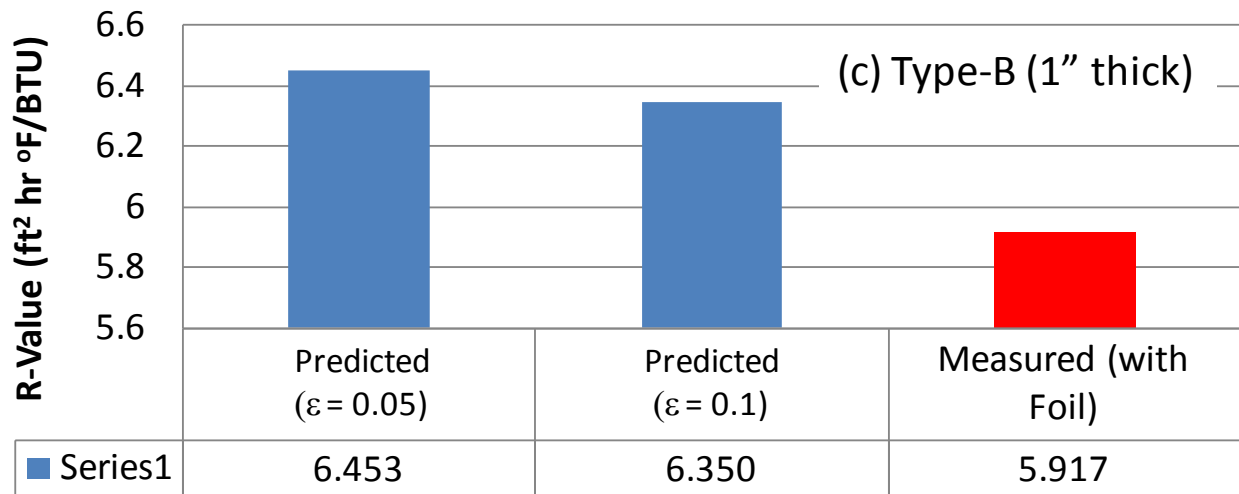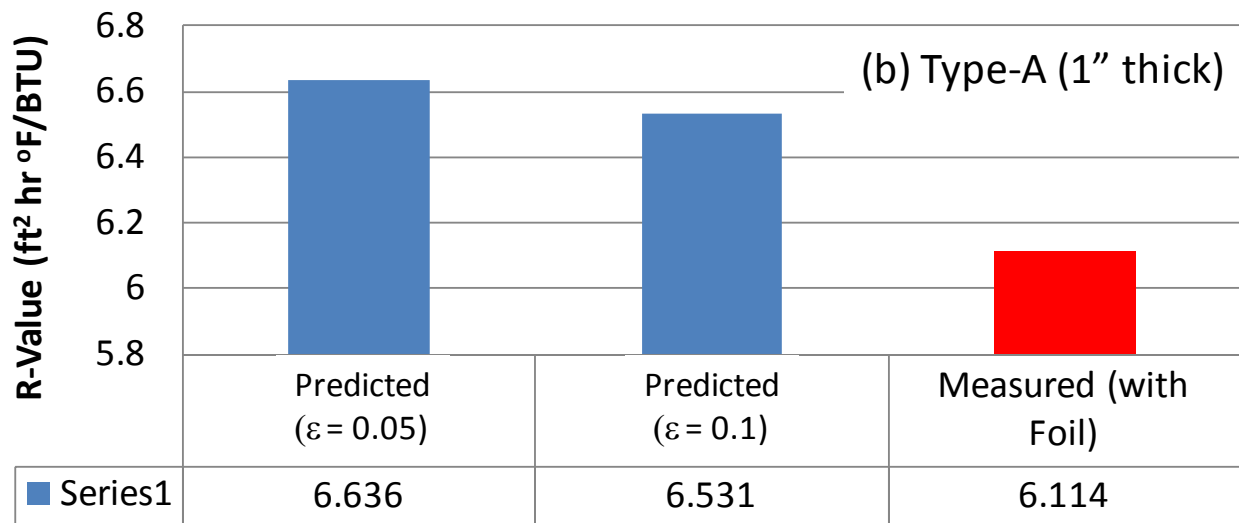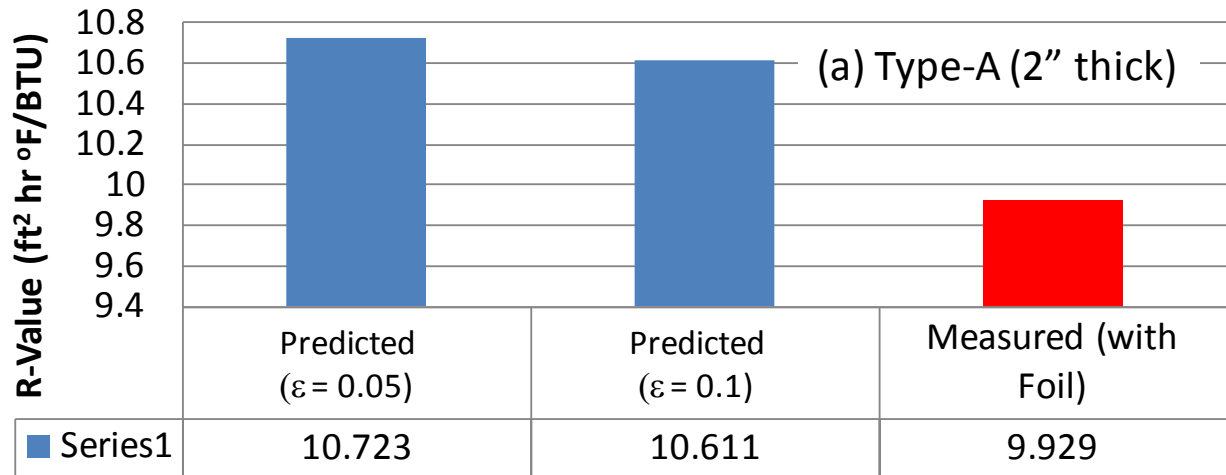**Figure 2.** Dependence of R-value on foil emissivity for sample stacks shown in Figure 1

**Figure 3.** Comparison between predicted R-values with foil emissivity of 0.05 and 0.1 and measured R-values [4] for sample stacks shown in Figure 1
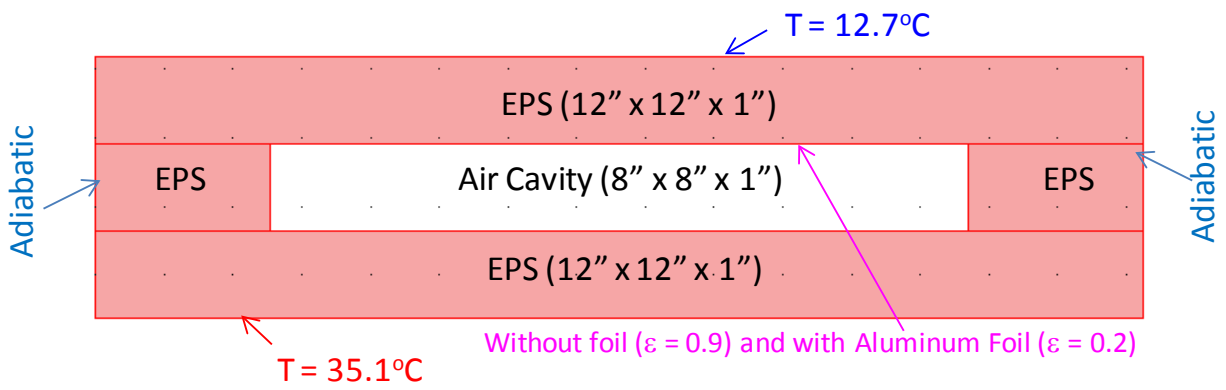
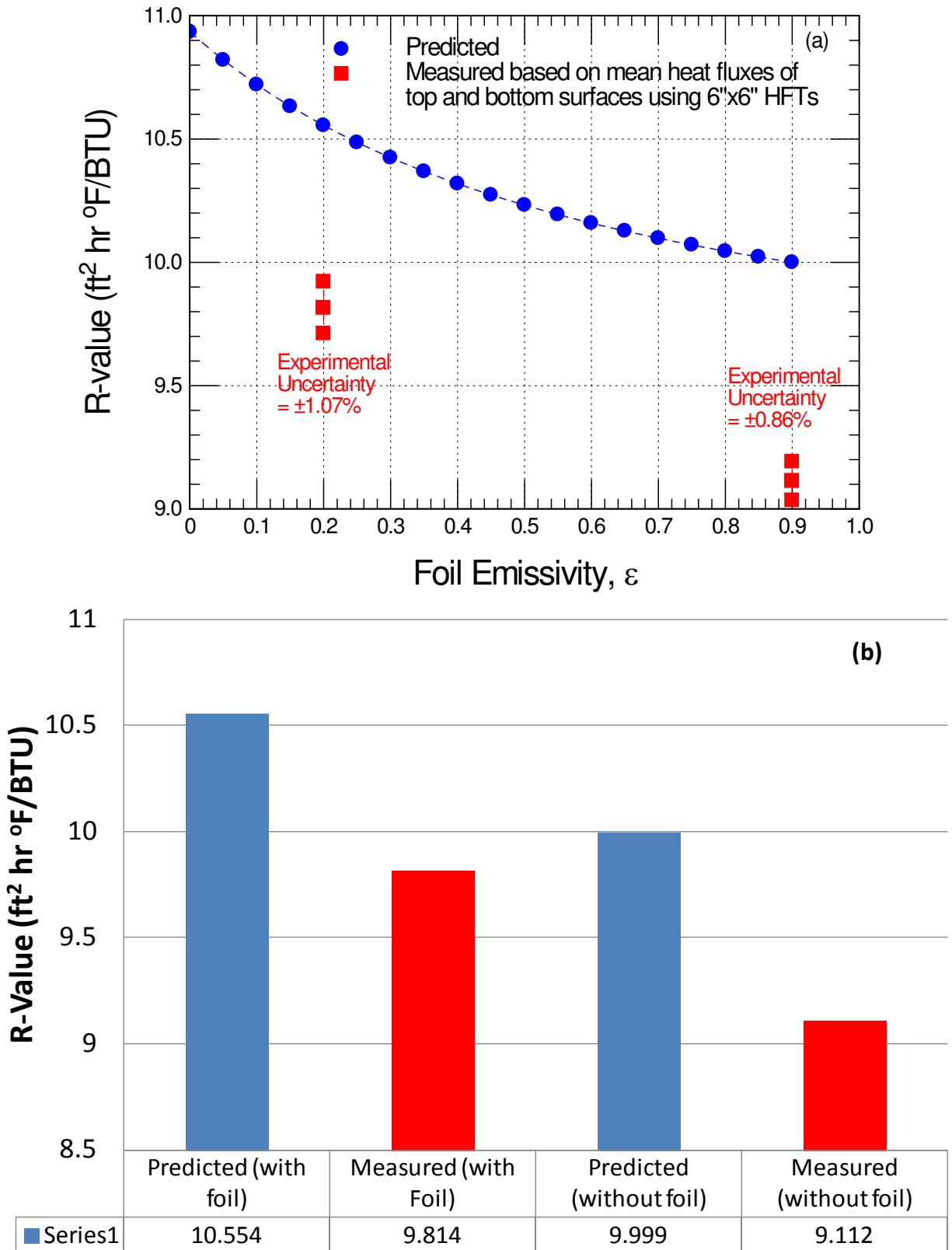**Figure 4.** Sample stacks tested at NRC (ASTM C-518 test method [12])

**Figure 5.** Comparison between the predicted and measured R-value of EPS sample stacks with and without foil
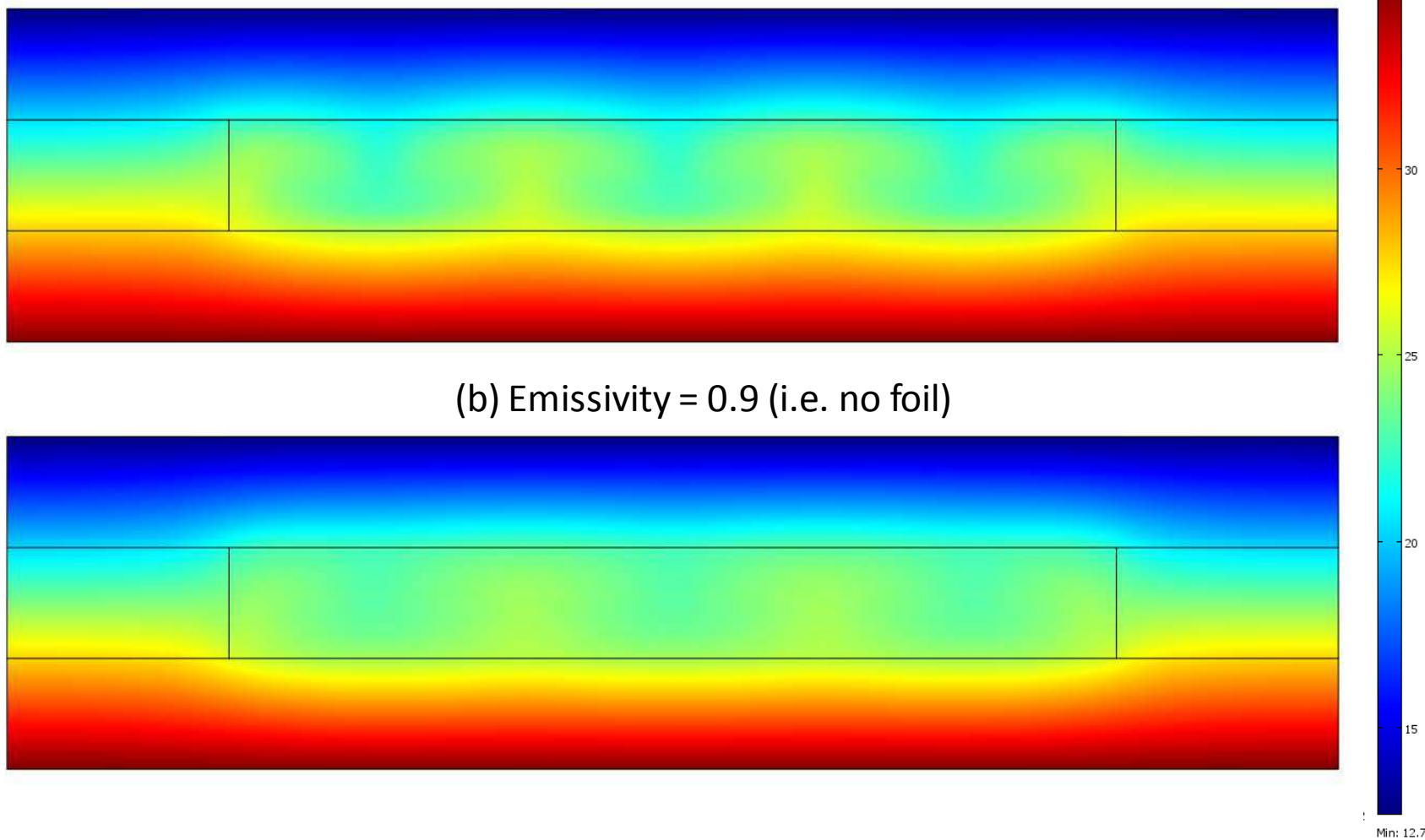
(a) Emissivity = 0.2 (aluminum foil)



(b) Emissivity = 0.9 (i.e. no foil)



**Figure 6.** Predicted temperature distribution (in $^{o}$C) in the sample stacks with and without foil
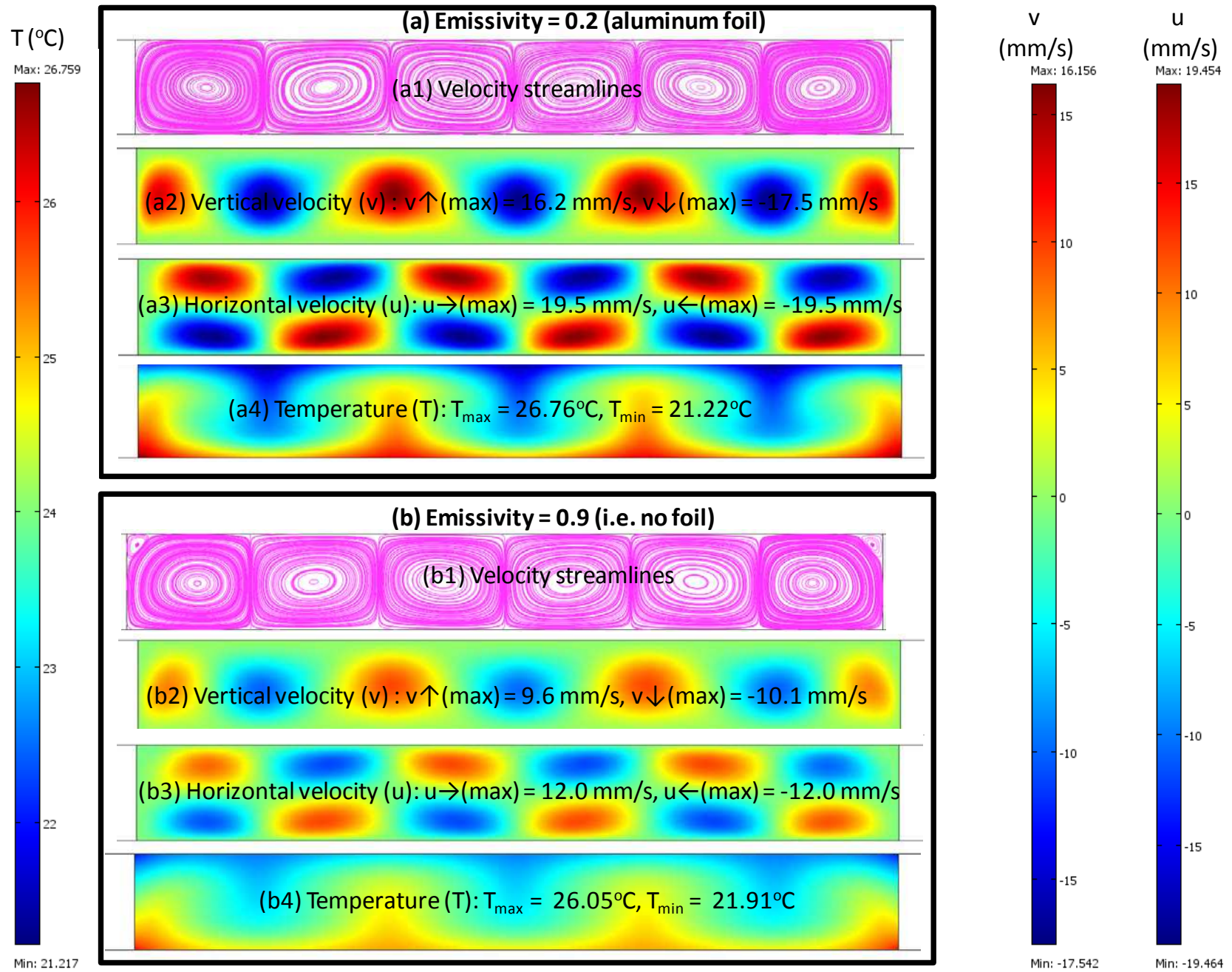
**(a) Emissivity = 0.2 (aluminum foil)**

(a1) Velocity streamlines

(a2) Vertical velocity (v) : v↑(max) = 16.2 mm/s, v↓(max) = -17.5 mm/s

(a3) Horizontal velocity (u): u→(max) = 19.5 mm/s, u←(max) = -19.5 mm/s

(a4) Temperature (T): $T_{max}$ = 26.76°C, $T_{min}$ = 21.22°C

**(b) Emissivity = 0.9 (i.e. no foil)**

(b1) Velocity streamlines

(b2) Vertical velocity (v) : v↑(max) = 9.6 mm/s, v↓(max) = -10.1 mm/s

(b3) Horizontal velocity (u): u→(max) = 12.0 mm/s, u←(max) = -12.0 mm/s

(b4) Temperature (T): $T_{max}$ = 26.05°C, $T_{min}$ = 21.91°C

T (°C)
Max: 26.759
26
25
24
23
22
Min: 21.217

v (mm/s)
Max: 16.156
15
10
5
0
-5
-10
-15
Min: -17.542

u (mm/s)
Max: 19.454
15
10
5
0
-5
-10
-15
Min: -19.464

**Figure 7.** Predicted velocity field and temperature distribution in the air cavity of sample stacks with and without foil
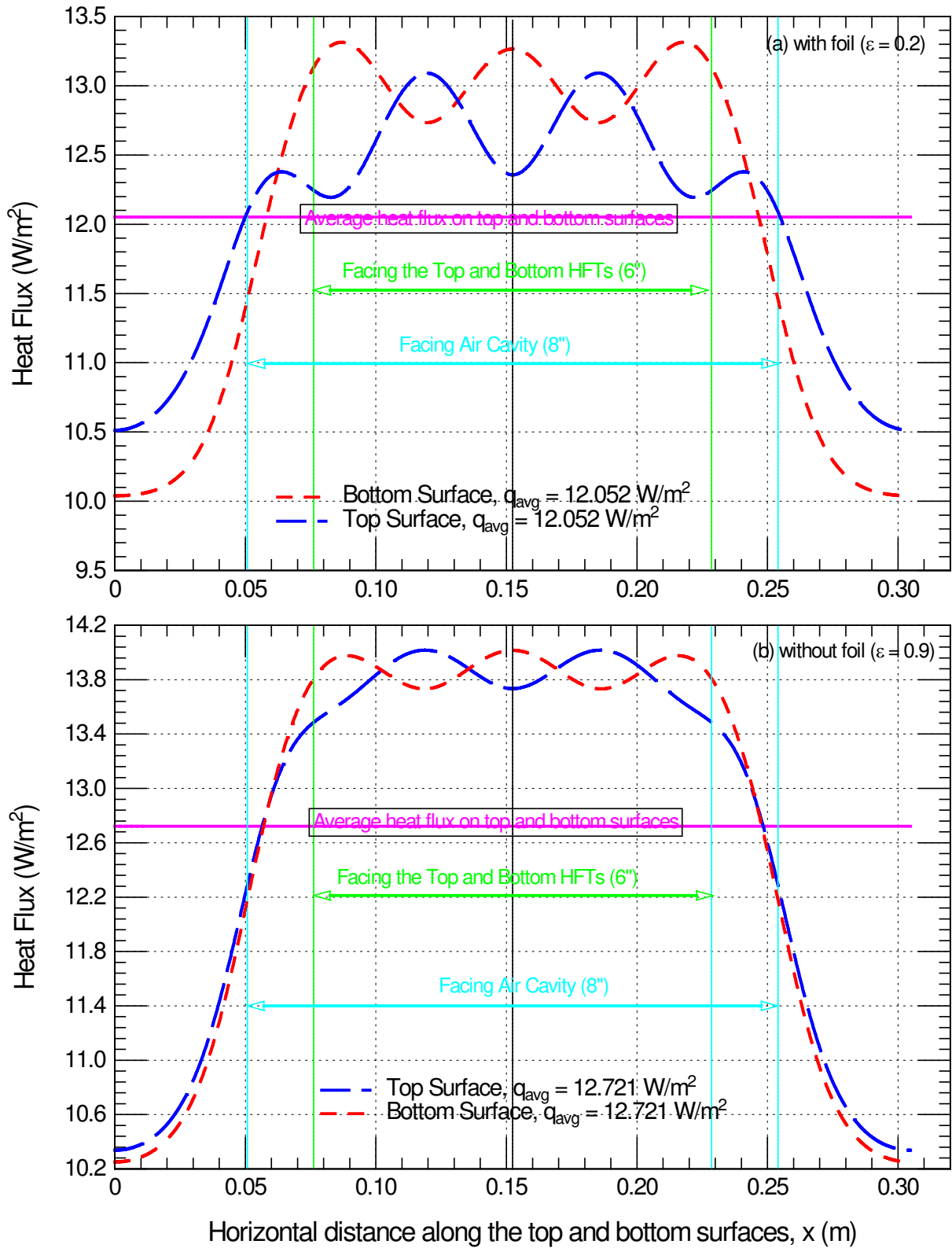
30

**Figure 8.** Predicted the local heat flux on the top and bottom surface of the sample stacks with and without foil
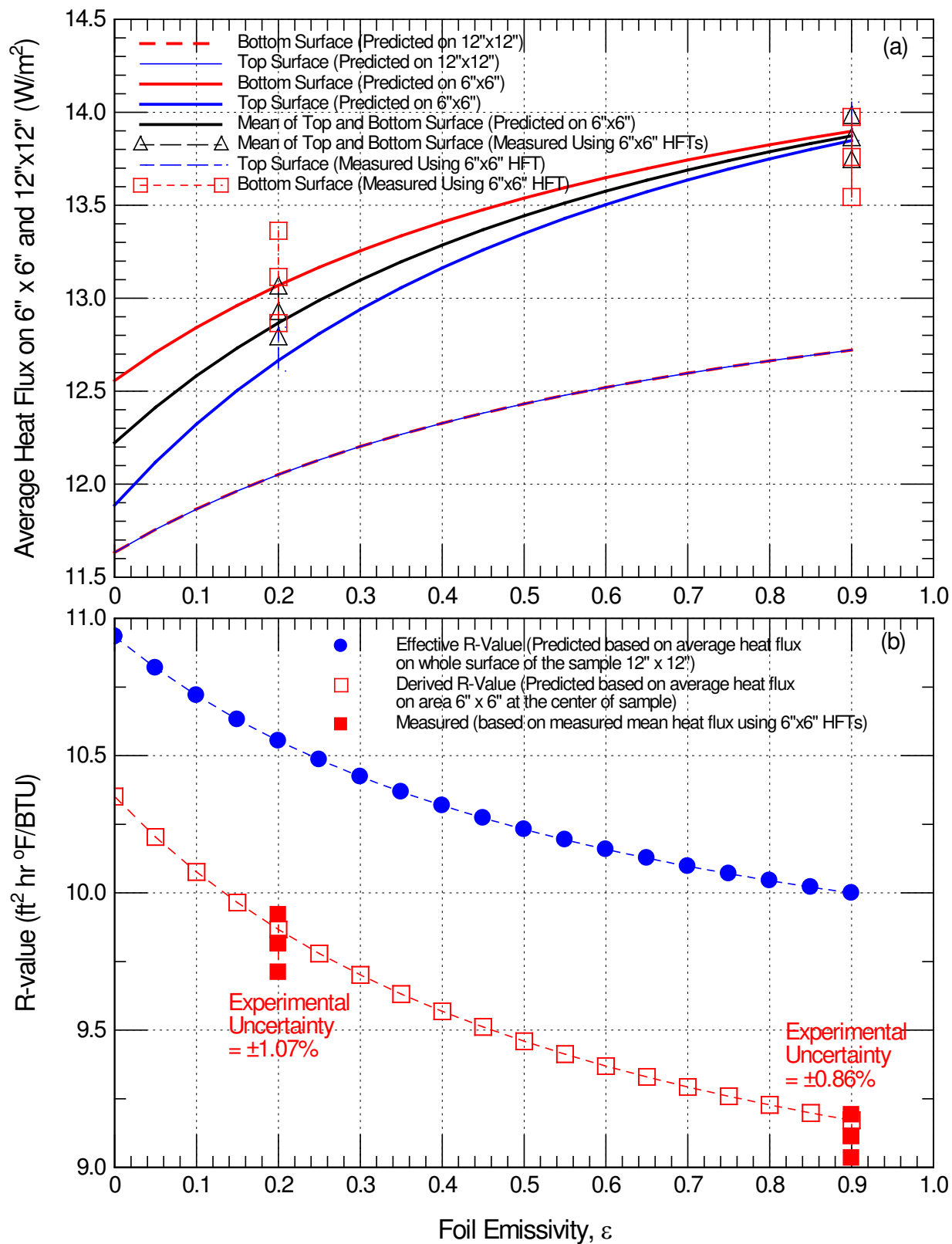
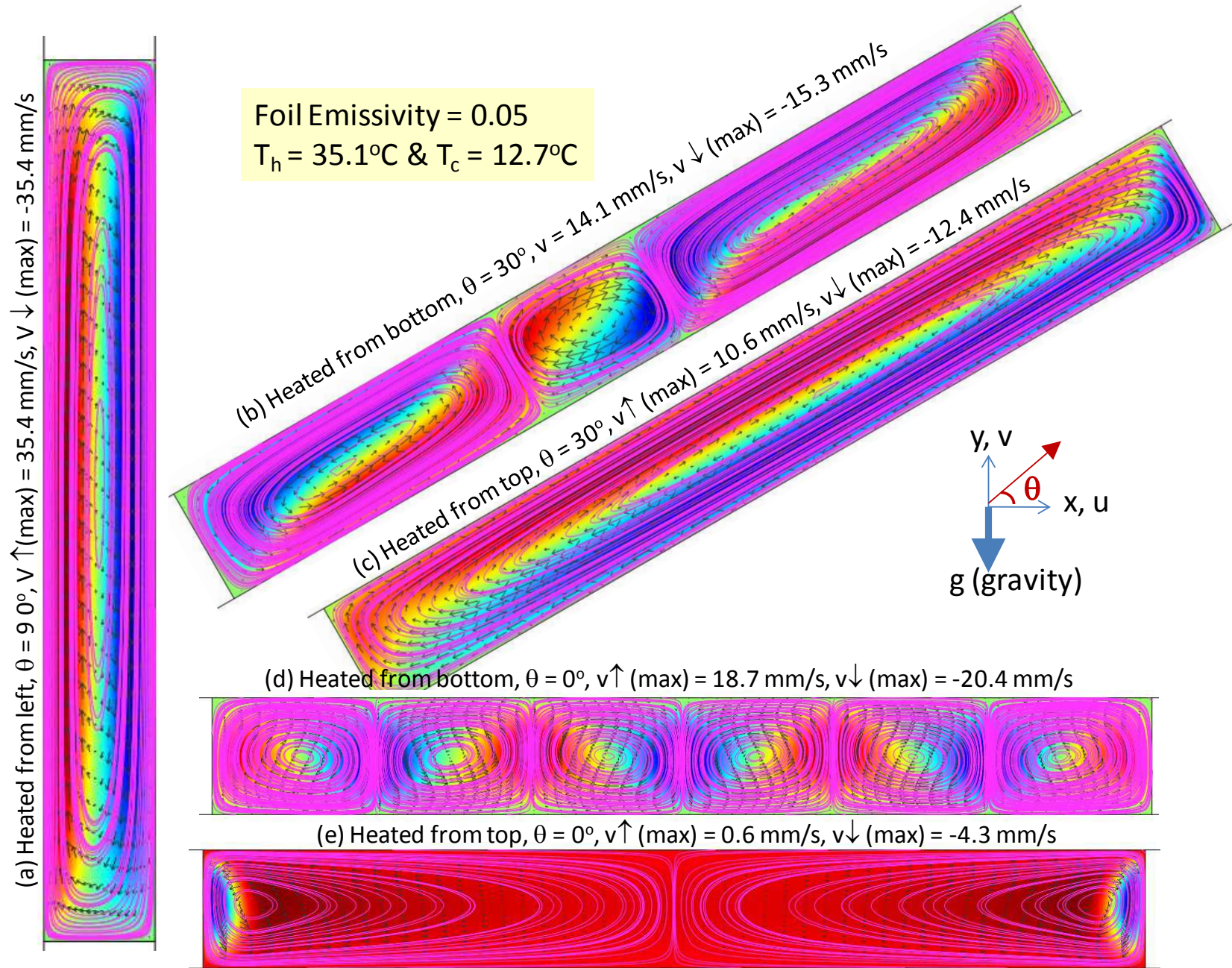**Figure 9.** Comparisons between predictions and measurements for sample stacks with and without foil

**Foil Emissivity = 0.05**
$T_h = 35.1^\circ C$ & $T_c = 12.7^\circ C$

(a) Heated from left, $\theta = 90^\circ$, $V\uparrow$ (max) = 35.4 mm/s, $V\downarrow$ (max) = -35.4 mm/s

(b) Heated from bottom, $\theta = 30^\circ$, $v = 14.1$ mm/s, $v\downarrow$ (max) = -15.3 mm/s

(c) Heated from top, $\theta = 30^\circ$, $v\uparrow$ (max) = 10.6 mm/s, $v\downarrow$ (max) = -12.4 mm/s

(d) Heated from bottom, $\theta = 0^\circ$, $v\uparrow$ (max) = 18.7 mm/s, $v\downarrow$ (max) = -20.4 mm/s

(e) Heated from top, $\theta = 0^\circ$, $v\uparrow$ (max) = 0.6 mm/s, $v\downarrow$ (max) = -4.3 mm/s

**Figure 10.** Vertical velocity contours and flow field in the air cavity of sample stacks with different inclinations
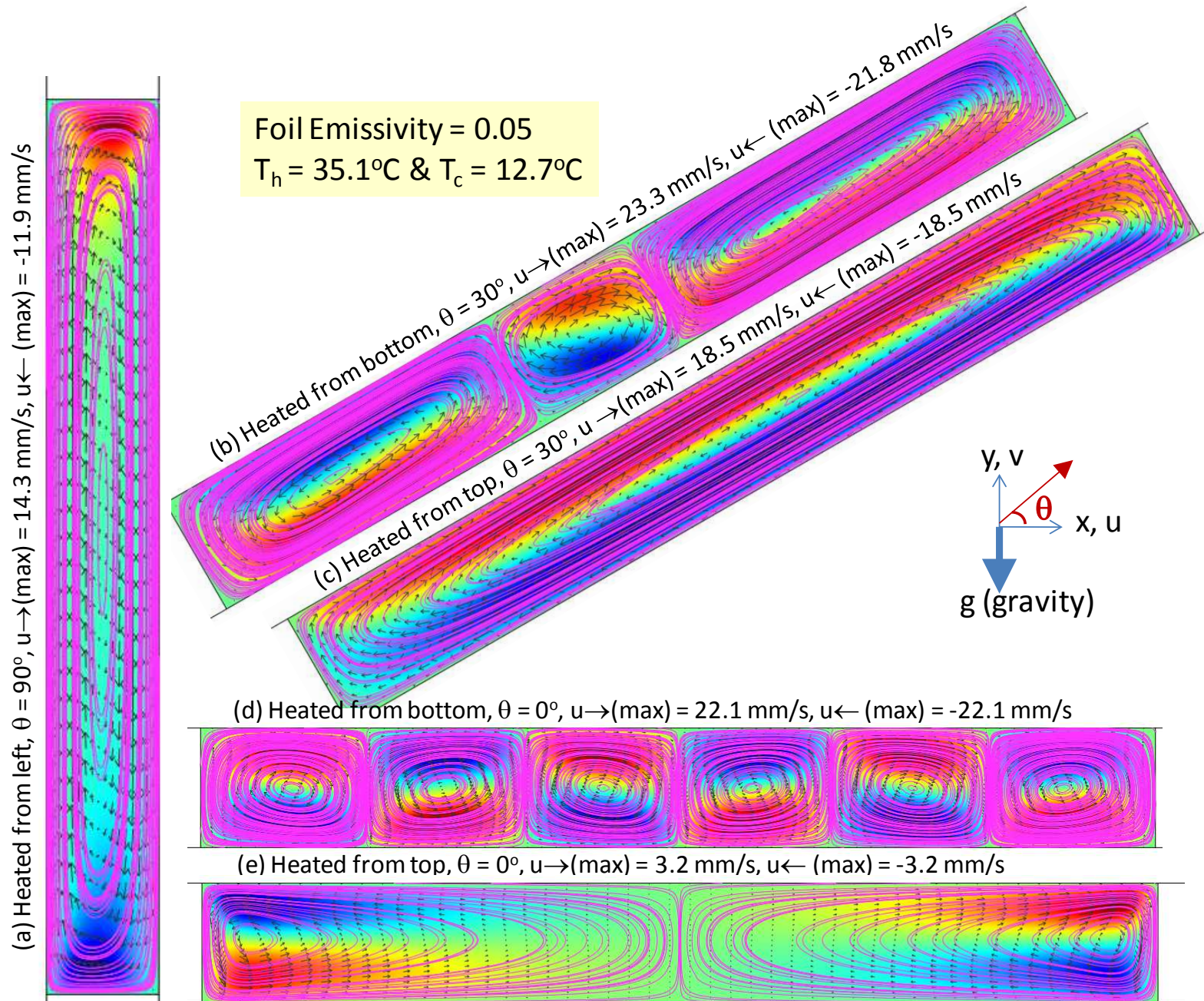
**Figure 11.** Horizontal velocity contours and flow field in the air cavity of sample stacks with different inclinations
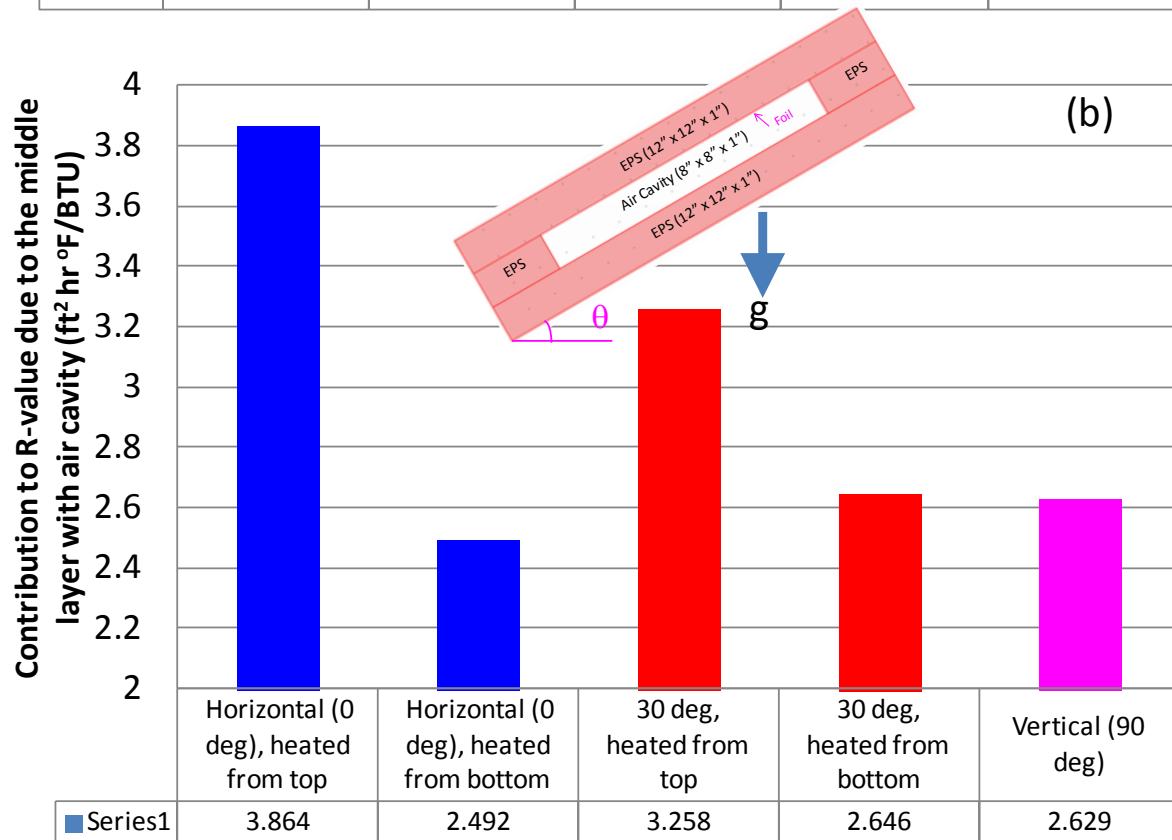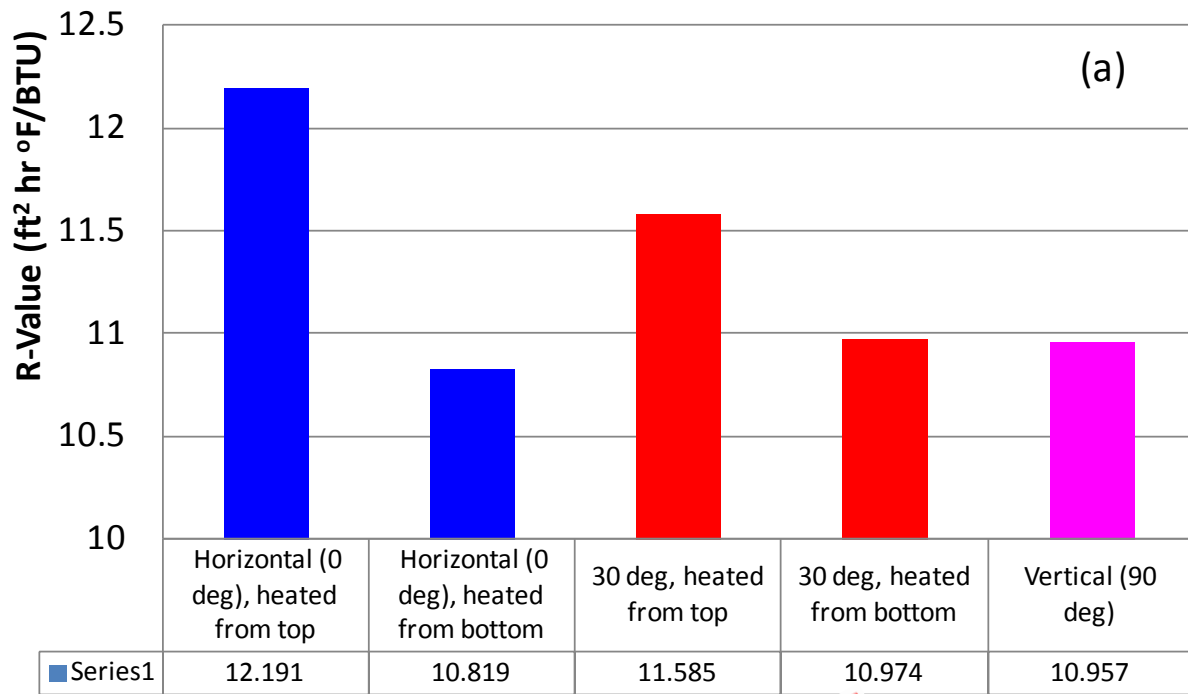
34

**Figure 12.** Effect of inclination angle of sample stack and direction of heat flow on the effective R-value in the case of foil emissivity of 0.05
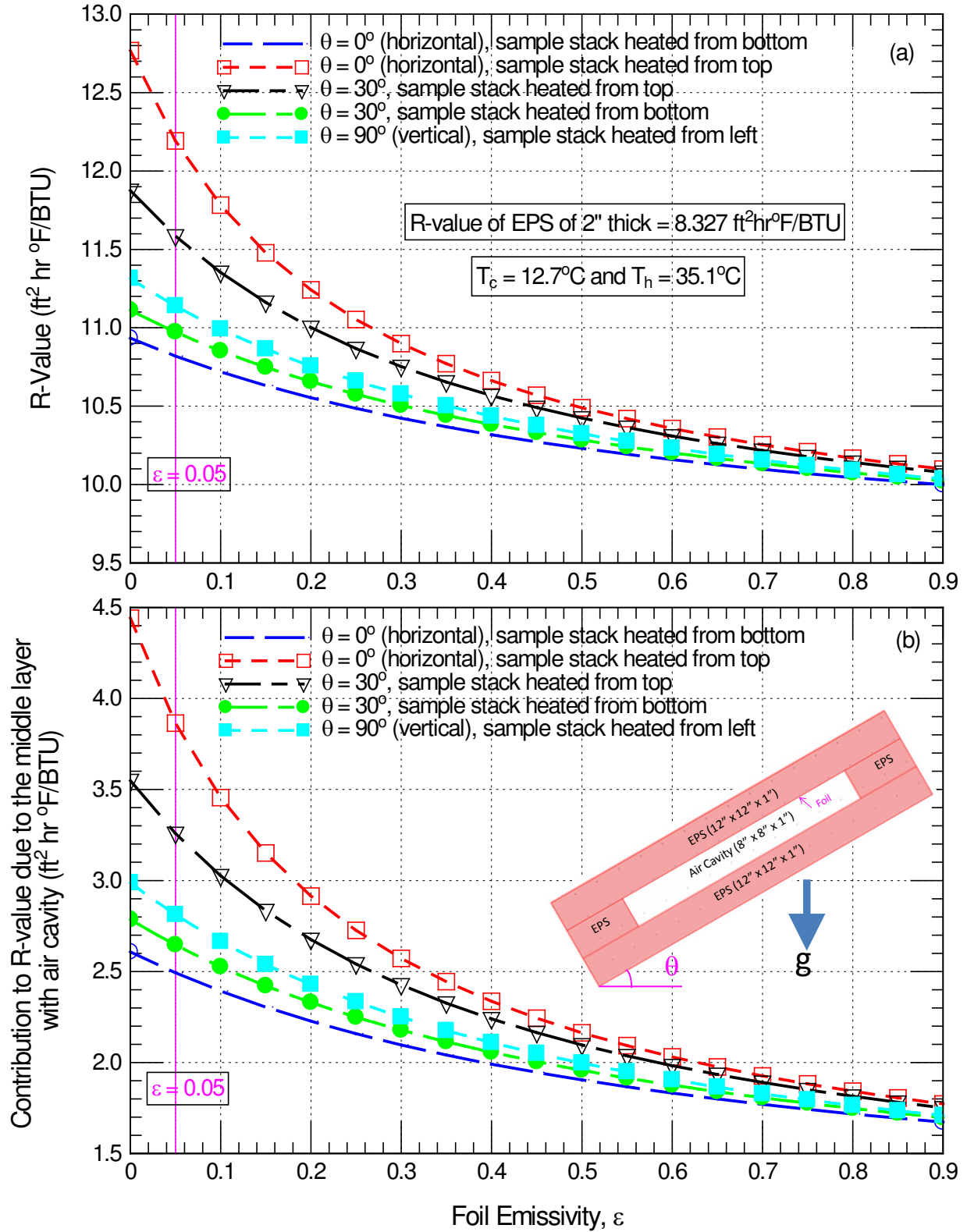
**Figure 13.** Effect of inclination angle of sample stack, foil emissivity and direction of heat flow on the effective R-value
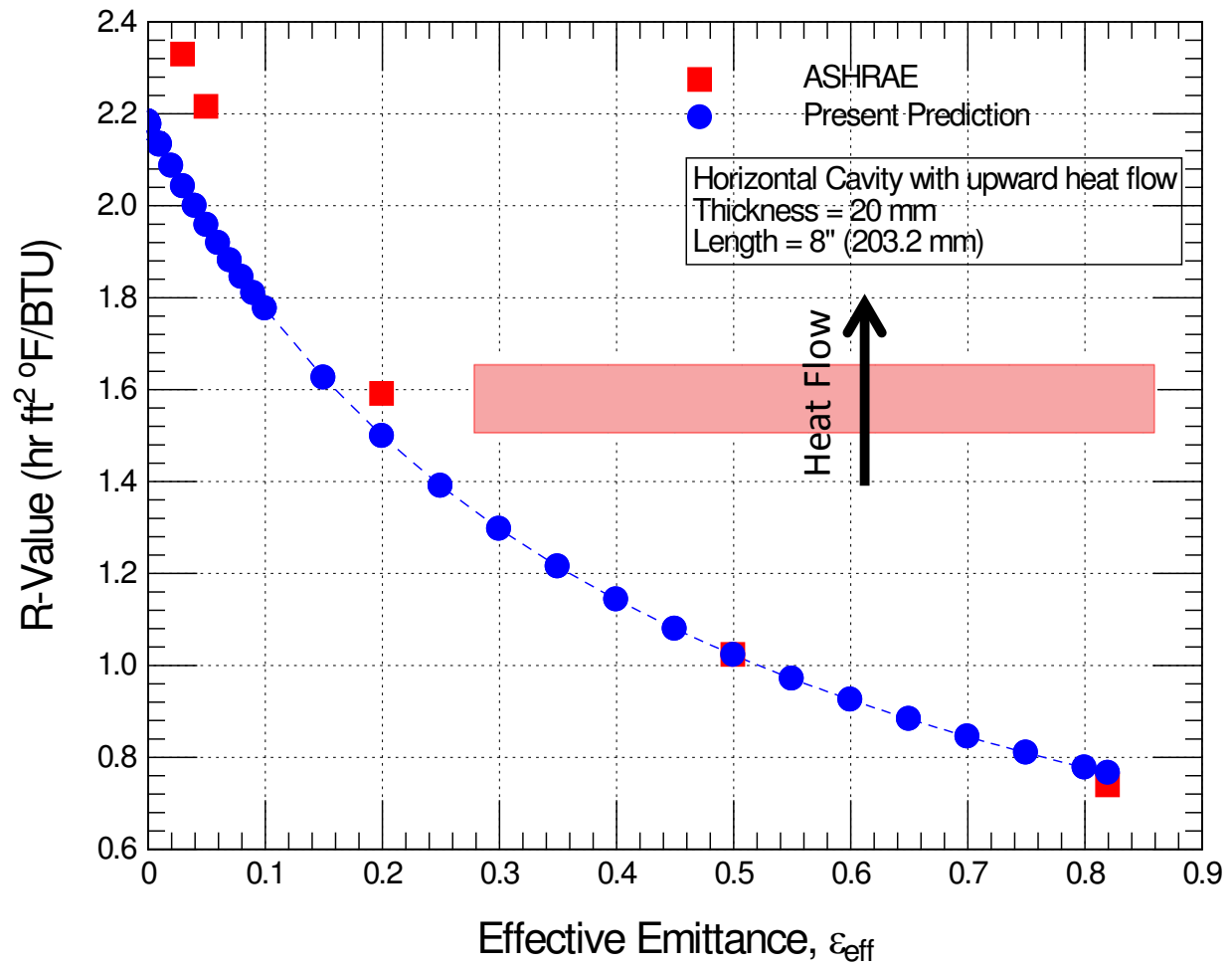
**Figure 14.** Comparison between the predicted and ASHRAE R-values for horizontal air cavity (20 mm thick and 8" (203.2) long) with different $\varepsilon_{eff}$ in the case of upward heat flow with $T_{mean}$ = 32.2$^{o}$C and $\Delta T$ = 5.6$^{o}$C
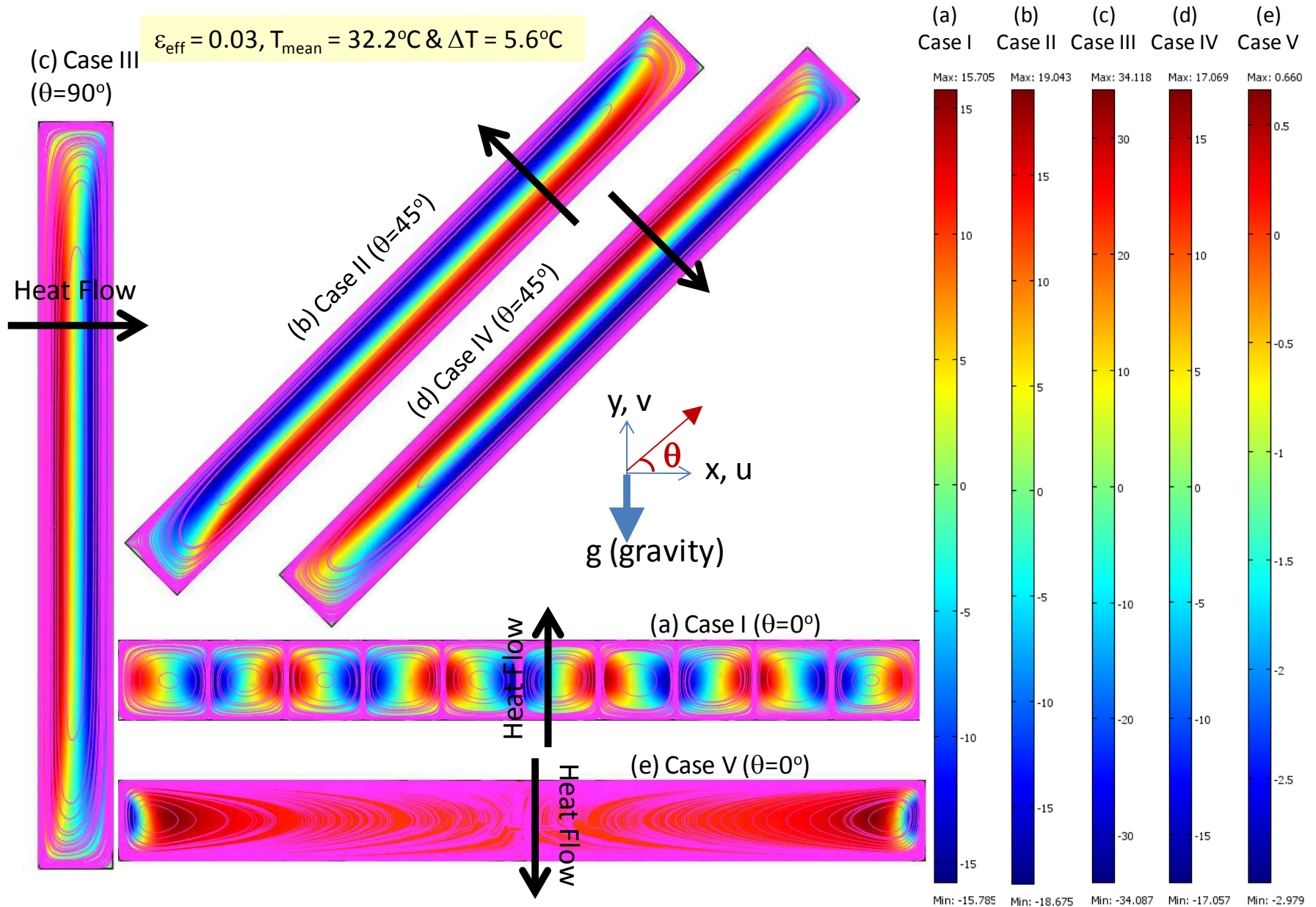
**Figure 15.** Vertical velocity contours (in mm/s) and streamlines in the air cavity (20 mm thick) with different inclinations and directions of heat flow for $\varepsilon_{eff} = 0.03$, $T_{mean} = 32.2^oC$ & $\Delta T = 5.6^oC$